
NEWMA: a new method for scalable model-free online change-point detection

Nicolas Keriven
École normale Supérieure
Paris, France
nicolas.keriven@ens.fr

Damien Garreau
Max Plank Institute for Intelligent Systems
Tübingen, Germany
damien.garreau@tuebingen.mpg.de

Iacopo Poli
LightOn
Paris, France
iacopo@lighton.io

Abstract

We consider the problem of detecting abrupt changes in the distribution of a multi-dimensional time series, with limited computing power and memory. In this paper, we propose a new method for model-free online change-point detection that relies only on fast and light recursive statistics, inspired by the classical Exponential Weighted Moving Average algorithm (EWMA). The proposed idea is to compute *two* EWMA statistics on the stream of data *with different forgetting factors*, and to compare them. By doing so, we show that we implicitly compare recent samples with older ones, without the need to explicitly store them. Additionally, we leverage Random Features to efficiently use the Maximum Mean Discrepancy as a distance between distributions. We show that our method is orders of magnitude faster than usual non-parametric methods for a given accuracy.

1 Introduction

The goal of online change-point detection is to detect abrupt changes in the distribution of samples in a data stream. One seeks to detect a change as soon as it occurs, while minimizing the number of false alarms. Online change-point detection has numerous practical applications, for instance medical monitoring via the segmentation of EEG, ECG and fMRI signals [30, 38, 6], or detections of changes in audio [5] or video [24, 1] streams. We refer to [32] for a more thorough review. In recent applications, the need arises to perform such methods on embedded devices, for instance in video streams from body-worn or surveillance video cameras [2], or on data collected by smart phones [22]. In addition to being constrained by limited power and memory, such personal devices collect data that can be potentially sensitive. Hence the need to process the stream locally without storing the data and sharing it with other machines.

Setting. We consider a stream of samples $(x_t)_{t \in \mathbb{N}}$ with values in \mathbb{R}^d with potentially large d . The goal of change-point detection is to detect changes in the distribution of the samples x_t . In this paper, we *design* our algorithms to be sensitive to variations of $\theta_\Psi(\pi) \stackrel{\text{def.}}{=} \mathbb{E}_{x \sim \pi} \Psi(x)$, where π is the distribution of the samples, and $\Psi : \mathbb{R}^d \rightarrow \mathcal{H}$ is a mapping to a normed space $(\mathcal{H}, \|\cdot\|)$ (generally, $\mathcal{H} = \mathbb{R}^m$ or \mathbb{C}^m). It covers most of the usual cases found in the literature: for instance, $\Psi = \text{Id}$, then $\theta_\Psi(\pi) = \mathbb{E}x$, and the methods studied in this paper aim to detect variations in the *mean* of the distribution of samples. When $\Psi : x \mapsto xx^\top$ and the samples have zero mean, $\theta_\Psi(\pi) = \text{Cov}(x)$, and we aim to detect changes in the covariance of the signal.

If the user has *prior knowledge* about which quantity $\theta_\Psi(\pi)$ is susceptible to change over time, then Ψ can be chosen accordingly. If not, we will see in Sec. 3 that a somewhat “universal” embedding can be obtained by taking Ψ as *kernel random features*.

Methods with prior knowledge. Historically, many methods for online change-point detection assume knowledge of the in-control distribution (that is, the situation before the change happens). They rely either on a (generalized) likelihood ratio test when the model is fully specified, or monitor changes in some statistic, for instance the empirical mean or the variance [11]. See the textbook by [3] and references therein.

The method proposed in this paper takes its inspiration in a classical approach called Exponential Weighted Moving Average (EWMA) [34], which we describe in Alg. 1 as follow¹. Recall that our goal is to monitor the quantity $\theta_\Psi(\pi) = \mathbb{E}_\pi \Psi(x)$ for some user-defined Ψ . Assuming that we know the *in-control* value of $\theta_\Psi(\pi)$, denoted by θ^* , EWMA computes *recursively* a weighted average of $\Psi(x_t)$, with exponential weights that favor the more recent samples. When this average deviates too much from θ^* , an alarm is raised. The exponential weights (instead of, say, uniform weights) reduce the detection delay, and increase robustness to potentially irrelevant data in the past.

Parametric methods such as EWMA are extremely fast and have low memory footprint, due to their recursive nature: when a new sample arrives, the cost of the update is essentially that of computing $\Psi(x)$ once. Moreover, they preserve data privacy, in the sense that they never store raw samples but only statistics computed from them, which are generally *not* one-to-one mappings. Nevertheless, they require prior knowledge, which severely limits their use.

Data: Stream of data x_t , function Ψ , in-control value θ^* , forgetting factor $0 < \Lambda < 1$, threshold $\tau > 0$, initial value \mathbf{z}_0

```

for  $t = 1, 2, \dots$  do
     $\mathbf{z}_t = (1 - \Lambda)\mathbf{z}_{t-1} + \Lambda\Psi(x_t)$ ;
    if  $\|\mathbf{z}_t - \theta^*\| \geq \tau$  then
        | Flag  $t$  as a change-point
    end
end

```

Algorithm 1: EWMA [34]

Methods without prior knowledge. To solve these problems, methods without prior knowledge were proposed, that do not make any assumption on the in-control situation. Some [21, 43] are two-steps adaptation of the previous approaches, with an in-control estimation phase followed by the detection itself. Others perform online estimation of a time-varying model[41, 8]. Finally, some methods are said *model-free*: they simply compare a pool of recent samples with samples that came before, using a metric that measures the difference between the distributions of the two batches [23, 28, 26]. In our settings, we describe an example of such an approach in Alg. 2, that we simply refer to as Moving Average² (MA). This algorithm compares an empirical average of $\Psi(x)$ over the last B samples with one computed on the B samples that came before. When the difference is significant, an alarm is raised.

Model-free methods are useful in a wide class of problems, since they can adapt to potentially any in-control situation. Despite these advantages, they are often computationally intensive and have a high memory footprint, since they store raw data that may be high dimensional (see Tab.1 in Sec. 2).

Contributions and outline. The main goal of this paper is to propose a method that gets the best of both worlds, that is, that does not store any raw data, like EWMA, while being simultaneously model-free like MA. To this end, in Sec. 2, we introduce “No-prior-knowledge” EWMA (NEWMA). We show that NEWMA implicitly compares pools of recent and old samples *without having to keep them in memory*, and derive a heuristic to choose its hyperparameters. In Sec. 3, we further instantiate the method and describe a possible “universal” embedding Ψ as a kernel feature map, and we show

¹Our description of EWMA is similar to the original, with the addition that the data are transformed by the mapping Ψ .

²While this simple algorithm appears several times in the literature [23, 27], as far as we know it does not have a designated name.

Data: Stream of data x_t , function Ψ , in-control value θ^* , forgetting factor $0 < \Lambda < 1$, threshold $\tau > 0$, initial value \mathbf{z}_0

Initialize $\mathbf{z}_{2B} = \frac{1}{B} \sum_{i=1}^B \Psi(x_i)$, $\mathbf{z}'_{2B} = \frac{1}{B} \sum_{i=1}^B \Psi(x_{B+i})$;

```

for  $t = 2B + 1, \dots$  do
   $\mathbf{z}_t = \mathbf{z}_{t-1} + \frac{1}{B} (\Psi(x_{t-B}) - \Psi(x_{t-2B}))$ ;
   $\mathbf{z}'_t = \mathbf{z}'_{t-1} + \frac{1}{B} (\Psi(x_t) - \Psi(x_{t-B}))$ ;
  if  $\|\mathbf{z}_t - \mathbf{z}'_t\| \geq \tau$  then
    | Flag  $t$  as a change-point
  end
end

```

Algorithm 2: MA (e.g., [23])

how it can be approximated with Random Features (RFs) [33]. In Section 4, we examine how to set the detection threshold. We first review two classical “parametric” approaches, which are however generally not applicable in practice in model-free situations, then propose a numerical procedure for computing on-the-fly a dynamic threshold τ , which empirically performs better than a fixed threshold. Experiments over synthetic and real data are presented in Sec. 5, where we take advantage of a sublinear construction of RFs [25] and, more strikingly, of a recent development in optical computing [35] that can compute RF in $\mathcal{O}(1)$ for any dimension d and number of features m . We show that our algorithm retrieves change-points at a given precision orders of magnitude faster than competing model-free approaches.

2 Proposed algorithm

Data: Stream of data x_t , function Ψ , forgetting factors $0 < \lambda < \Lambda < 1$, threshold $\tau > 0$, initial value $\mathbf{z}_0 = \mathbf{z}'_0$

```

for  $t = 1, 2, \dots$  do
   $\mathbf{z}_t = (1 - \Lambda)\mathbf{z}_{t-1} + \Lambda\Psi(x_t)$ ;
   $\mathbf{z}'_t = (1 - \lambda)\mathbf{z}'_{t-1} + \lambda\Psi(x_t)$ ;
  if  $\|\mathbf{z}_t - \mathbf{z}'_t\| \geq \tau$  then
    | Flag  $t$  as a change-point
  end
end

```

Algorithm 3: NEWMA (proposed)

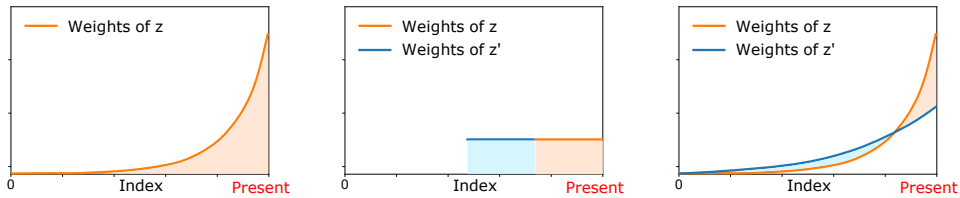


Figure 1: Weights used in the empirical average computations in EWMA (top left), MA (top right), and NEWMA (bottom) algorithms as a function of time. In orange (resp. blue), the weights associated to the average \mathbf{z}_t (resp. \mathbf{z}'_t).

In this section we introduce the proposed algorithm, NEWMA (Alg. 3), and give some theoretical properties.

NEWMA is based on the following idea: compute **two EWMA statistics with different forgetting factors** $\lambda < \Lambda$, and raise an alarm when these two statistics are too far apart. The intuition behind this idea is simple: the statistic with the larger forgetting factor Λ gives “more importance” to recent samples than the one that uses λ , so the distance between them should increase in case of a recent change.

Table 1: Computational and memory footprint of the main algorithms discussed in this article. C_Ψ (resp. M_Ψ) indicates time complexity (resp. the memory requirement) of computing Ψ . In Scan- B , N is the number of windows of size B considered.

ALGO.	TIME	MEM.
EWMA (Alg. 1)	$C_\Psi + m$	$m + M_\Psi$
<i>Model-free:</i>		
MA (Alg. 2)	$C_\Psi + m$	$Bd + m + M_\Psi$
Scan- B [26]	NBd	NBd
NEWMA (Alg. 3)	$C_\Psi + m$	$m + M_\Psi$

To help illustrate this, in Fig. 1, we schematically represent the three different weighting procedures of EWMA, MA and NEWMA. As mentioned in the introduction: 1) EWMA computes recursively one average with exponential weights, but requires prior knowledge of a control value to compare with; 2) MA computes averages in two different time windows, but needs to keep in memory the last $2B$ samples for this purpose; and 3) by recursively computing two exponentially weighted averages with different forgetting factors, NEWMA compares pools of recent and old samples, but does not need to store them in memory. In Table 1, we compare their computational costs, including the model-free Scan- B algorithm of [26] which we will use in our experiments. We can see that the complexity of MA and Scan- B is dominated by the storage of the high-dimensional data, while NEWMA has the same complexity than EWMA. A crucial factor is the computational cost of Ψ , see Sec. 3 for the case of kernel random features.

In this section, we first prove basic properties of NEWMA, then provide a useful heuristic for the choice of the two forgetting factors Λ, λ .

Related work. The idea of using several forgetting factors in recursive updates has been proposed before, for instance in the so-called Multivariate EWMA (MEWMA) [29, 22], which uses a different factor for each coordinate of multivariate data, or to optimize the detection over different time-scales [19]. The statistic computed by NEWMA is different: it compute the *difference* of two recursive averages with distinct forgetting factors, in order to extract time-varying information. To the best of our knowledge, the key idea behind NEWMA has not been proposed before.

2.1 First properties

Let us formalize the intuition behind NEWMA.

Proposition 1 (Rewriting the detection statistic). Define $B \stackrel{\text{def.}}{=} \left\lceil \frac{\log(\Lambda/\lambda)}{\log((1-\lambda)/(1-\Lambda))} \right\rceil$, and run NEWMA (Alg. 3). Then, for any $t > B$,

$$\mathbf{z}_t - \mathbf{z}'_t = C \left(\sum_{i=t-B+1}^t a_i \Psi(x_i) - \left(b_0 \mathbf{z}_0 + \sum_{i=1}^{t-B} b_i \Psi(x_i) \right) \right),$$

where $C = C(\lambda, \Lambda, B) \stackrel{\text{def.}}{=} (1-\lambda)^B - (1-\Lambda)^B \in (0, 1)$, and a_i, b_i are positive numbers which depend only on Λ and λ , such that $\sum_{i=t-B+1}^t a_i = 1$ and $\sum_{i=0}^{t-B} b_i = 1$. The exact expressions of a_i and b_i can be found in App. A.1.

We see that NEWMA computes the difference between an empirical average of $\Psi(x_i)$ over the last B samples (where B depends on Λ and λ) and an empirical average over the samples that came before. The weights a_i and b_i are positive and sum to 1.

Using Prop. 1 and simple concentration inequalities, we can show basic probabilistic bounds on the detection statistic. Recall that we designed our algorithm to detect changes through the lens of $\theta_\Psi(\pi) = \mathbb{E}\Psi(x)$. Hence, for any π, π' , we define the pseudometric

$$d_\Psi(\pi, \pi') \stackrel{\text{def.}}{=} \|\mathbb{E}_\pi \Psi(x) - \mathbb{E}_{\pi'} \Psi(x)\|,$$

which quantifies how “different” two distributions are in terms of $\theta_\Psi(\pi)$. The following proposition shows simple “pointwise” bounds on $\mathbf{z}_t - \mathbf{z}'_t$ under the null or when there is a change in the last

B samples. We note that such pointwise results are different from usual quantity examined in change-point detection such as the mean time between false alarm, which will be examined later.

Proposition 2 (Bounds at a given time). *Suppose that $M \stackrel{\text{def.}}{=} \sup_{x \in \mathbb{R}^d} \|\Psi(x)\| < \infty$. Let $t > B$ be a fixed time point, and $\rho \in (0, 1)$ be some probability of failure.*

(i) *Assume that all samples x_1, \dots, x_t are drawn i.i.d. from π . Then, with probability at least $1 - \rho$, we have*

$$\|\mathbf{z}_t - \mathbf{z}'_t\| \lesssim \varepsilon_1 + \varepsilon_2, \quad (1)$$

where $\varepsilon_1 = M\sqrt{(\Lambda + \lambda)\log(1/\rho)}$ and $\varepsilon_2 = [(1 - \lambda)^t - (1 - \Lambda)^t] \|\mathbf{z}_0 - \mathbb{E}_\pi \Psi(x)\|$.

(ii) *Assume that the last B samples are drawn i.i.d. from a distribution π' , and all the samples that came before are drawn i.i.d. from π (that is, $x_{t-B}, \dots, x_t \stackrel{\text{i.i.d.}}{\sim} \pi'$ and $x_1, \dots, x_{t-B} \stackrel{\text{i.i.d.}}{\sim} \pi$). Then, with probability at least $1 - \rho$ on the samples, we have*

$$\|\mathbf{z}_t - \mathbf{z}'_t\| \gtrsim Cd_\Psi(\pi, \pi') - \varepsilon_1 - \varepsilon_2. \quad (2)$$

Prop. 2 shows that, when no change occurs (under the null) the detection statistic is bounded with high probability, and when the last B samples are distributed “differently” from the previous ones, it is greater than a certain value with high probability. As expected, this difference is measured in terms of the pseudometric d_Ψ . Note that a more precise statement can be found in the supplementary material.

Remark 3. *For the sake of clarity, in Prop. 2, (ii), we assumed that exactly the last B samples were drawn from π' , and that all samples that came before were drawn from π . In App. A.2, we show a more general result which examines the case where less than B recent samples are drawn from π' , and proves robustness to irrelevant data in the far past.*

2.2 Choice of the forgetting factors Λ and λ

Although the role of the hyperparameters (Λ, λ) in the NEWMA algorithm is simple to understand intuitively, it is not clear how to set their values at this stage. On the contrary, the window size B has a more interpretable meaning: it is the number of recent samples compared with old ones. In this section, we derive a simple heuristic to set both parameters (Λ, λ) for a given B , built upon the theoretical results of the previous section. We note that choosing a forgetting factor for EWMA can be difficult [10].

Our starting point is expression of the window size B derived in Prop. 1. We first note that a possible parameterization of NEWMA is through B and *one* of the forgetting factors, say Λ : if $\Lambda > \frac{1}{B+1}$, there is a unique $\lambda = \lambda_{\Lambda, B} \leq \frac{1}{B+1}$ such that $\frac{\log(\Lambda/\lambda)}{\log((1-\lambda)/(1-\Lambda))} = B$ in Prop. 1. Indeed, $f : x \mapsto x(1-x)^B$ is increasing on $[0, \frac{1}{B+1}]$ and decreasing on $[\frac{1}{B+1}, 1]$, so the equation $f(x) = f(\Lambda)$ has exactly one solution in $[0, 1]$ besides Λ itself. Thus λ is uniquely defined by (B, Λ) . We now turn to the choice of Λ given B .

From Prop. 2, we can see that the null hypothesis is intuitively distinguishable from the alternative if the bound under the null (1) is smaller than the guaranteed deviation (2) when there is a change, that is, $\varepsilon_1 + \varepsilon_2 \leq Cd_\Psi(\pi, \pi') - \varepsilon_1 - \varepsilon_2$, which is equivalent to

$$d_\Psi(\pi, \pi') \gtrsim (\varepsilon_1 + \varepsilon_2)/C.$$

Since we want our algorithm to be sensitive to the smallest possible change in $d_\Psi(\pi, \pi')$, the previous reasoning suggest that a good choice for Λ is to minimize the right-hand side of this expression. To obtain our final heuristic, we replace $\|\mathbf{z}_0 - \mathbb{E}_\pi \Psi(x)\|$ by the upper bound $2M$ in the expression of ε_2 , and we take $t = 2B$; since $\varepsilon_2 \xrightarrow[t \rightarrow \infty]{} 0$ and intuitively we consider that our algorithm must be “applicable” as soon as we have received twice the window size in data.

In definitive, for a fixed B , we propose the following heuristic to choose³ Λ :

$$\Lambda^* = \arg \min_{\Lambda \in (\frac{1}{B+1}, 1)} \frac{\sqrt{\lambda_{\Lambda, B} + \Lambda} + (1 - \lambda_{\Lambda, B})^{2B} - (1 - \Lambda)^{2B}}{(1 - \lambda_{\Lambda, B})^B - (1 - \Lambda)^B},$$

³Note that we discard the multiplicative constants as well as $\log \frac{1}{\rho}$, which we found to have negligible effect in practice.

where we recall that $\lambda_{\Lambda, B}$ is the unique λ such that $\frac{\log(\Lambda/\lambda)}{\log((1-\lambda)/(1-\Lambda))} = B$, and $\lambda^* = \lambda_{\Lambda^*, B}$. In practice, Λ^* and λ^* do not have explicit expressions with respect to B but they can easily be approximated by one-dimensional optimization schemes.

3 Choice of Ψ : Random Features

Let us now turn to the important choice of the embedding Ψ . We recall that Ψ is user-defined, and that the algorithms studied in this paper are sensitive to variations in the quantity $\theta_\Psi(\pi) = \mathbb{E}_\pi \Psi(x)$. As mentioned before, if the practitioner knows in advance which statistic is susceptible to vary, then Ψ can be chosen accordingly. However, one does not necessarily have a priori knowledge on the nature of the change. In this section, we describe a somehow “universal” embedding related to kernel metric on distributions.

For most Ψ , $d_\Psi(\pi, \pi')$ is only a pseudometric on probability distributions: for instance, when $\Psi(x) = x$, it can only distinguish distributions that have different means. Ideally however, one would like d_Ψ to be a true metric, that is, we want $d_\Psi(\pi, \pi') = 0$ if, and only if, $\pi = \pi'$. Unfortunately, for any mapping Ψ with values in a finite-dimensional space, d_Ψ cannot be a true metric—otherwise $\theta_\Psi(\cdot)$ would be an isometry between an infinite-dimensional space and a finite-dimensional space. In particular, this is the case for any Ψ used in practice. Luckily, as described in the rest of this section, an interesting strategy is to leverage the Random Features methodology to obtain *random* embeddings Ψ such that $d_\Psi(\pi, \pi')$ approximates a true metric between distributions *with high probability*.

Maximum Mean Discrepancy. A possible choice for such a metric is the Maximum Mean Discrepancy (MMD, [16]). Given a positive definite kernel κ on \mathbb{R}^d , take \mathcal{H} as the reproducing kernel Hilbert space associated to K . If we set $\Psi(x) = \kappa(x, \cdot)$ and $\|\cdot\| = \|\cdot\|_{\mathcal{H}}$, then, in our notation, $d_\Psi(\pi, \pi') = \|\mathbb{E}_\pi \kappa(x, \cdot) - \mathbb{E}_{\pi'} \kappa(x, \cdot)\|_{\mathcal{H}}$ is the MMD between π and π' , that we denote by $\text{MMD}(\pi, \pi')$. When the kernel K is *characteristic*, it is a true metric. Many conditions have been formulated over the years for K to be characteristic [37], and for instance the Gaussian kernel is characteristic. First introduced in the context of two-sample test, the MMD appears quite naturally in the context of kernel change-point detection [20, 15, 26].

Random Features. In practice, since $\Psi(x) = \kappa(x, \cdot)$ cannot be stored in memory to compute the theoretical MMD, empirical estimates thereof are used. Such estimates usually make use of the so-called *kernel trick*, and require the computation of a U -statistic depending on populations drawn from both distributions: it is for instance the method used in the kernel Scan- B algorithm [26]. Since we do not want to store samples when NEWMA is running, least of all perform costly computations on these samples, we resort to kernel Random Features (RF, [33]), since *the Euclidean distance between averaged random features approximates the MMD with high probability over the features*. RFs and MMD have been combined together before, for accelerating the estimation of the MMD [39] or as a mean to design random projections of distributions in an inverse-problem context [18]. We also note that alternatives to RFs have been studied in the MMD literature [9], which is an interesting path for future work.

Let us briefly describe the RF machinery. Assume that the kernel κ can be written as $\kappa(x, x') = \mathbb{E}_{\omega \sim \Gamma} \phi_\omega(x) \overline{\phi_\omega(x')}$ for a family of functions $\phi_\omega : \mathbb{R}^d \rightarrow \mathbb{C}$ parameterized by $\omega \in \mathbb{R}^q$, and a probability distribution Γ on \mathbb{R}^q . This is for instance the case for all translation-invariant kernels [4]. Drawing m parameters $\omega_1, \dots, \omega_m \stackrel{i.i.d.}{\sim} \Gamma$, the RF paradigm consists in defining $\Psi : \mathbb{R}^d \rightarrow \mathbb{C}^m$ as

$$\Psi(x) \stackrel{\text{def.}}{=} \frac{1}{\sqrt{m}} (\phi_{\omega_j}(x))_{j=1}^m, \quad (3)$$

and taking $\|\cdot\|$ as the classical Hermitian norm on \mathbb{C}^m . A simple computation (see the proof of Prop. 4 in App. A.2) then shows that $d_\Psi(\pi, \pi') \approx \text{MMD}(\pi, \pi')$, with high probability over the ω_j . With this choice of Ψ , we have the following result similar to Prop. 2.

Proposition 4. *Suppose that $\sup_{x, \omega} |\phi_\omega(x)| \leq M$. Define $\Psi(\cdot)$ as in Eq. (3). Let $\rho \in (0, 1)$ be a probability of failure. Suppose that the assumptions of Prop. 2, (ii) hold. Then, with probability at least $1 - 2\rho$ on both samples x_i and parameters ω_j , it holds that*

$$\|\mathbf{z}_t - \mathbf{z}'_t\| \geq C \left(\text{MMD}^2(\pi, \pi') - \varepsilon_m \right)_+^{\frac{1}{2}} - \varepsilon_1 - \varepsilon_2, \quad (4)$$

where $(x)_+ = \max(x, 0)$ and $\varepsilon_m = \frac{2\sqrt{2}M^2}{\sqrt{m}} \sqrt{\log \frac{1}{\rho}}$.

By the previous proposition, if the MMD between π and π' is large, then with high probability so is the deviation of $\|\mathbf{z}_t - \mathbf{z}'_t\|$. The additional error $\sqrt{\varepsilon_m}$ is of the order of the previous error ε_1 if $m = \mathcal{O}((\Lambda + \lambda)^{-2})$.

Choice of kernel κ . The choice of a good kernel κ is a notoriously difficult problem. Ideally, one would choose it so as to maximize $\text{MMD}(\pi, \pi')$, however neither π nor π' are known in advance in our setting. In practice, we use the Gaussian kernel. Having access to some initial training data, we choose the bandwidth σ using the median trick as in [26]. We leave for future work more involved methods for kernel selection [42].

Fast random features and computational cost. A crucial factor in the application of NEWMA is the complexity of the mapping Ψ . For usual Random Fourier Features (RFF) [33], computing $\Psi(x)$ requires storing the dense matrix of frequencies ω_j , and performing a costly matrix-vector product. However, a large body of work is dedicated to accelerate the computation of such random features. For instance, the Fastfood approximation [25] reduces the time complexity to $\mathcal{O}(m \log d)$ and memory to $\mathcal{O}(m)$. More strikingly, in [35], the authors build an Optical Processing Unit (OPU) that computes random features in $\mathcal{O}(1)$ and eliminates the need to store the random matrix. We recall the respective complexities of these three approaches in Table 2.

Table 2: Time complexity C_Ψ and memory requirement M_Ψ for different Random Features schemes.

	RFF	FF	OPU
C_Ψ	$\mathcal{O}(md)$	$\mathcal{O}(m \log d)$	$\mathcal{O}(1)$
M_Ψ	$\mathcal{O}(md)$	$\mathcal{O}(m)$	$\mathcal{O}(1)$

4 Setting the threshold

In this section, we go back to the case of any general mapping Ψ . An important question for any change-point detection method that tracks a statistic along time is how to set the threshold τ above which a change-point is detected. In this section, we begin by adapting to NEWMA two classical approaches that use the property of the algorithm under the null hypothesis. However, while they are interesting in their own right, these approaches generally cannot be directly used in practice since they require to know the in-control distribution π . Hence we describe an efficient numerical procedure to dynamically adapt the threshold during a continuous run with multiple changes.

4.1 Convergence under the null

A first approach to set the threshold τ is to derive the distribution of $\|\mathbf{z}_t - \mathbf{z}'_t\|$ under the null, and set τ to obtain a desired probability of exceeding it. In this section, we derive an asymptotic result on the distribution of this statistic when $\lambda \rightarrow 0$ and $t \rightarrow \infty$. Unlike Prop. 2, where Ψ is assumed uniformly bounded, it relies on the slightly weaker assumption that Ψ has a finite fourth order moment.

Theorem 5 (Convergence under the null). *Assume $c = \Lambda/\lambda > 1$ is fixed, and let $\Lambda \rightarrow 0$, with $t \geq \frac{2}{\lambda} \log \frac{1}{\lambda}$. Assume that all samples x_i are drawn i.i.d. from π . Suppose that $\mathbb{E}_\pi \|\Psi(x)\|^4 < +\infty$. Set $\mu = \mathbb{E}_\pi \Psi(x)$, and $K(x, x') = \langle \Psi(x) - \mu, \Psi(x') - \mu \rangle_{\mathcal{H}}$. Define the eigenvalues and eigenvectors of K in $L^2(\pi)$, i.e., define $\xi_\ell \geq 0$ and $\psi_\ell \in L^2(\pi)$ such that $K(x, x') = \sum_{\ell \geq 1} \xi_\ell \psi_\ell(x) \psi_\ell(x')$ and $\langle \psi_\ell, \psi_{\ell'} \rangle_{L^2(\pi)} = 1_{\ell=\ell'}$. Then,*

$$\frac{1}{\lambda} \|\mathbf{z}'_t - \mathbf{z}_t\|^2 \xrightarrow[\eta \rightarrow 0]{\mathcal{L}} Y \stackrel{\text{def.}}{=} \frac{(1-c)^2}{2(1+c)} \sum_{\ell \geq 1} \xi_\ell W_\ell^2, \quad (5)$$

where $(W_\ell)_{\ell \geq 1}$ is an infinite sequence of independent standard normal random variables.

The proof follows closely [36] (Sec. 5.5.2) adapted to our setting, with the use of a multivariate version of Lindeberg's central limit theorem (Th. 12 in the Appendix) instead of the classical Central Limit Theorem. Th. 5 allows to set the threshold τ if the eigenvalues ξ_ℓ are (approximately) known,

for instance they can be estimated using the Gram matrix of K on training data [17], which we leave for future work. In Fig. 2 (left panel), we illustrate the result on a toy example.

4.2 Mean time between false alarms

Another classical method to set the threshold τ is to adjust a desired mean time between false alarms under the null, defined as $\bar{T} \stackrel{\text{def.}}{=} \mathbb{E} [\inf \{t \mid t \text{ is flagged}\}]$, where the expectation is over the samples under the null. In the literature, it is sometimes referred to as the Average Run Length (ARL) under control. We show in App. B that, in some cases, it is possible to adapt the Markov chain-based proof developed for classical EWMA by [13] to NEWMA. Unlike the results from the previous sections, our analysis is valid without any boundedness assumption on Ψ or its moments. The statement of the result (Th. 8) and its proof, rather technical, are deferred to App. B, where we also derive additional computations in the case where $\Psi(x) \in \mathbb{R}$.

In simple cases, one can use Th. 8 to approximately compute \bar{T} . In Fig. 2 (right panel) we compare \bar{T} for NEWMA and EWMA on such an example, using respectively Th. 8 and the original approach by [13], as well as numerical simulations. For both algorithms we see that the theoretical expression closely matches the empirical observations. Like the previous approach, when the in-control distribution π is not known, Th. 8 cannot be directly applied. In some cases [26], one can obtain an asymptotic expression for \bar{T} which does not depend on π , which we leave for future work.

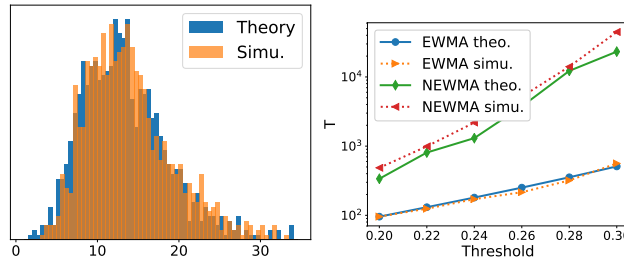


Figure 2: **Left:** Distribution of $\frac{1}{\lambda} \|\mathbf{z}_t - \mathbf{z}'_t\|^2$ when $\lambda \rightarrow 0$ as predicted by Th. 5, on a toy example. Namely, π is the uniform distribution on $[0, 1]$ and $\Psi(x) = [\sqrt{\xi_\ell} \psi_\ell(\cdot)]_{\ell=1}^{30}$ is defined as a collection of eigenfunctions $\psi_\ell(x) = \sqrt{2} \cos(2\pi\ell x)$, where the eigenvalues $(\xi_\ell)_{\ell=1}^{30}$ are randomly generated. We perform 1000 simulations of both Eq. (5) and NEWMA with $\Lambda = 2 \cdot 10^{-2}$, $\lambda = 10^{-2}$. **Right:** Comparison of the theoretical and observed values of \bar{T} for NEWMA (resp. EWMA) with respect to τ , with $\pi = \mathcal{N}(0, 1)$, $\Psi(x) = x$, $\Lambda = 2 \cdot 10^{-1}$ and $\lambda = 10^{-1}$. The simulations are averaged over 1000 runs, the theoretical expression is obtained with Th. 8 in App. B (resp. [13]) with a grid of precision $\varepsilon = 2 \cdot 10^{-2}$.

4.3 In practice: adaptive threshold

The two classical strategies presented above are generally not applicable in practice, since we do not know the in-control distribution π . Some statistics that compare sets of samples exhibits some properties that do not depend on the null distribution [23], however they are not directly applicable in the NEWMA framework and we leave their exploration under memory constraints for future work. We derive an efficient online numerical heuristic instead.

Consider *any* online change-point detection method based on a statistic $S_t \geq 0$ maintained in a streaming fashion, such that t is flagged if S_t exceeds a threshold $\tau > 0$: for instance, in the case of MA or NEWMA we have $S_t = \|\mathbf{z}_t - \mathbf{z}'_t\|$, Scan- B [26] and many other approaches also fit in this framework.

We propose here to let the threshold τ be also time-varying. More precisely, we make it follow the values of the statistic S_t “by above,” such that S_t exceeds the threshold only if it increases *abruptly*. This is done by maintaining a weighted average \bar{S}_t of the previous values of S_t recursively: $\bar{S}_t = (1 - \eta)\bar{S}_{t-1} + \eta S_t$, and defining the threshold above this average by scaling it: $\tau_t = a\bar{S}_t$ with $a > 1$. A time-point is then flagged when $S_t \geq \tau_t$. Empirically, we found this adaptive threshold procedure to be far more flexible than a fixed threshold. In our experiments, we found that setting

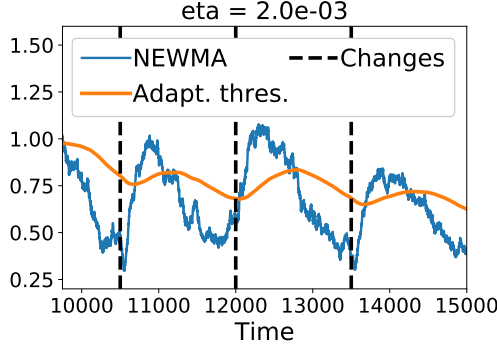


Figure 3: Illustration of the adaptive threshold procedure. The dotted line indicate a change, the blue line is the NEWMA statistic $\|z_t - z'_t\|$, and in yellow line is the adaptive threshold computed online as described in Sec. 4.3.

$\eta = \frac{1}{2}\lambda$ performs empirically well, however we note that such a choice is somewhat arbitrary and we leave the development of a heuristic, and possible theoretical analysis, for future work.

5 Experiments

In this experimental section we compare several model-free approaches: NEWMA where Ψ is one of the three different random features schemes described in Sec. 3: classical RFFs [33], FF [25], or OPU [35], the MA algorithm with RFFs, and the Scan- B algorithm [26]. Scan- B is implemented with a Gaussian kernel K , the other methods with RFs that correspond to the same kernel, except when using the OPU, for which the RFs and corresponding kernel are imposed by the optical hardware [35]. For all experiments we use a window size $B = 250$, and set the forgetting factors Λ^* and λ^* for NEWMA are then set according to Sec. 2.2. Following Prop. 4, the number of random features m is selected as $\mathcal{O}((\Lambda^* + \lambda^*)^{-2})$ (with a multiplicative constant $\frac{1}{4}$), except when using the OPU, for which, since we do not have any computational limits in this case, m is selected as 10 times this value. The bandwidth of the Gaussian kernel σ^2 is chosen using the median trick over the first 100 points in the time series, as in [26]. By default, the synthetic data are in dimension $d = 100$. The experiments run on a laptop with an Intel Core i7-7600U 2.80GHz. We make the code available in the supplementary material.

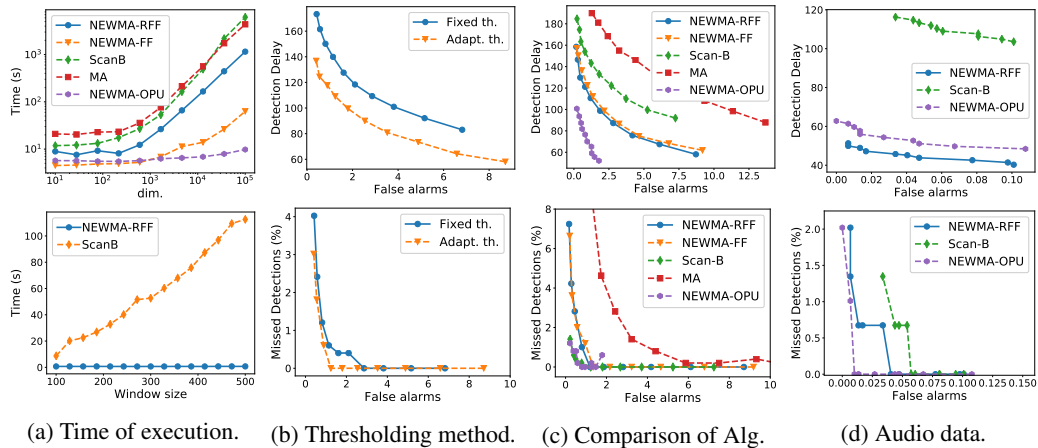


Figure 4: Experimental results. Unless otherwise specified, all algorithms are run with their default values described in Sec. 5. **Far Left:** Time of execution w.r.t dimension or window size. **Left:** Comparison of thresholding methods for NEWMA-RF on synthetic data. **Right:** Comparison of the three algorithms on synthetic data. **Far Right:** Application to audio data for Voice Activity Detection.

Time of execution. In Fig. 4a we examine the time of execution of the three algorithms with respect to the dimension d of the data and window size B . Being similar, Scan- B and MA have

approximately the same running time. As expected, NEWMA-FF is sublinear in the dimension, and NEWMA-OPU is almost independent of the dimension and much faster than the other approaches in high dimension. The results also confirm that NEWMA’s complexity is independent of B , while that of Scan- B increases linearly with B .

Results on synthetic data. Next we examine the detection performance of the three algorithms on synthetic data. We generate the data as follows: 10^6 samples are drawn from Gaussian Mixture Models (GMM) with $k = 10$ components, and the GMM changes every 2000 samples (at each change, we draw k new vector means according to a centered Gaussian distribution, k new covariance matrices from an inverse-Wishart distribution, and k new mixing weights from a Dirichlet distribution). In total, there are 500 changes to detect. We say that a change is detected when a non-flagged sample is followed by a flagged one. To evaluate performance, in the 1000 samples before every true change, we count every detected change as a false alarm, and in the 1000 samples after every true change, we record the time until the first detected change as detection delay. We then average these two quantities over the 500 changes. If no change is detected, we record a missed detection. We plot different ratios Expected Detection Delay (EDD)-to-False Alarms or Missed Detections-to-False Alarms by varying the multiplicative constant a in the adaptive threshold procedure.

In Fig. 4b we examine the effect of using the adaptive threshold instead of a fixed threshold. The adaptive procedure is superior to the fixed one, which cannot adapt to several changes in a single run.

In Fig. 4c we compare the algorithms. We first observe that MA performs generally poorly, confirming the superiority of Scan- B as a window-based approach. NEWMA with Gaussian random features (RFF or FF) exhibits a reduced detection delay compared to Scan- B but a slightly higher number of missed detections. NEWMA-OPU is seen to perform well, which may indicate that the kernel induced by the OPU is more appropriate than a Gaussian kernel on this example.

Results on real data. We apply our method to a Voice Activity Detection (VAD) task on audio data. We consider real environments background noise from the QUT-NOISE dataset [12] and add, every 10s, a 3s speech extract from the TIMIT dataset [14], with -7.5 dB Signal-to-Noise Ratio. Our goal is to detect the onset of the speech segments. We use the Short Time Fourier Transform of the signal. The data is $d = 129$ -dimensional, with a change every 1250 samples, for 300 changes in total. We take a window size $B = 150$. We display the results in Fig. 4d. Similar to the results on synthetic data, Scan- B has a higher detection delay than NEWMA. However, it does also exhibit slightly more missed detections: we suspect that, because it uses several windows of reference in-control samples, Scan- B is sensitive to highly heterogeneous data, which can be the case for audio data. In this case, the Gaussian random features are seen to perform on par with the OPU kernel.

6 Conclusion and outlooks

We introduced NEWMA, a new method for online change-point detection that is orders of magnitude faster and lighter than existing model-free methods. The key idea behind NEWMA is to compare recursive averages computed with different forgetting factors on the same data, in order to extract time-varying information without keeping in memory the raw data.

In the future, we plan to further develop the analysis of our method under the null to derive properties that do not depend on the in-control distribution, as done by [26]. Another direction for our research is the study of mappings Ψ for graph data, which, combined with NEWMA, would allow to detect changes in large-scale social networks [31]. Finally, density estimation from random feature moments [18] would allow extracting more information from $\mathbf{z}_t - \mathbf{z}'_t$ than mere occurrence of a change, such as the region of space in which the change occurred.

Acknowledgments

This work was funded in part by the CFM-ENS chair *Modèles et Sciences des Données*.

References

- [1] A. Abou-Elailah, V. Gouet-Brunet, and I. Bloch. Detection of abrupt changes in spatial relationships in video sequences. In *International Conference on Pattern Recognition Applications and Methods*, pages

- 89–106. Springer, 2015.
- [2] S. Allen, D. Madras, and Y. Ye. Change-point Detection Methods for Body-Worn Video. *arXiv:1610.06453*, 2016.
 - [3] M. Basseville and I. V. Nikiforov. *Detection of Abrupt Changes*, volume 2. Prentice-Hall, Inc., Upper Saddle River, NJ, USA, 1993.
 - [4] C. Berg, J. Christensen, and P. Ressel. Harmonic analysis on semigroups. 100, 1984.
 - [5] A. Bietti, F. Bach, and A. Cont. An online em algorithm in hidden (semi-) markov models for audio segmentation and clustering. In *Acoustics, Speech and Signal Processing (ICASSP)*, pages 1881–1885. IEEE, 2015.
 - [6] M. Bosc, F. Heitz, J. P. Armspach, I. Namer, D. Gounot, and L. Rumbach. Automatic change detection in multimodal serial mri: application to multiple sclerosis lesion evolution. *NeuroImage*, 20 2:643–56, 2003.
 - [7] S. Boucheron, G. Lugosi, and P. Massart. *Concentration inequalities: A nonasymptotic theory of independence*. Oxford University Press, 2013.
 - [8] Y. Cao, L. Xie, Y. Xie, and H. Xu. Sequential Change-Point Detection via Online Convex Optimization. *Entropy*, 20(2):108, 2018.
 - [9] K. Chwialkowski, A. Ramdas, D. Sejdinovic, and A. Gretton. Fast Two-Sample Testing with Analytic Representations of Probability Measures. In *Advances in Neural Information Processing Systems (NIPS)*, 2015.
 - [10] P. Čisar and S. M. Čisar. Optimization methods of EWMA statistics. *Acta Polytechnica Hungarica*, 8(5): 73–87, 2011.
 - [11] A. F. B. Costa and M. A. Rahim. A Single EWMA Chart for Monitoring Process Mean and Process Variance. *Quality Technology and Quantitative Management*, 3(3):295–305, 2006.
 - [12] D. Dean, S. Sridharan, R. Vogt, and M. Mason. The QUT-NOISE-TIMIT corpus for the evaluation of voice activity detection algorithms. In *Proceedings of Interspeech*, number September, pages 26–30, 2010.
 - [13] J. C. Fu, F. A. Spiring, and H. Xie. On the average run length of quality control schemes using a Markov Chain approach. *Statistics & Probability Letters*, 56(4):369–380, 2002.
 - [14] J. S. Garofolo, L. F. Lamel, W. M. Fisher, J. G. Fiscus, D. S. Pallett, N. L. Dahlgren, and V. Zue. TIMIT Acoustic-Phonetic Continuous Speech Corpus LDC93S1, 1993.
 - [15] D. Garreau and S. Arlot. Consistent change-point detection with kernels. *arXiv:1612.04740*, pages 1–41, 2016.
 - [16] A. Gretton, K. M. Borgwardt, M. J. Rasch, B. Schölkopf, and A. J. Smola. A Kernel Method for the Two-Sample Problem. In *Advances in Neural Information Processing Systems (NIPS)*, pages 513–520, 2007.
 - [17] A. Gretton, K. Fukumizu, Z. Harchaoui, and B. K. Sriperumbudur. A Fast, Consistent Kernel Two-Sample Test. In *Advances in Neural Information Processing Systems (NIPS)*, pages 673–681, 2009.
 - [18] R. Gribonval, G. Blanchard, N. Keriven, and Y. Traonmilin. Compressive Statistical Learning with Random Feature Moments. *arXiv:1706.07180*, 2017.
 - [19] D. Han, F. Tsung, X. Hu, and K. Wang. CUSUM and EWMA multi-charts for detecting a range of mean shifts. *Statistica Sinica*, 17(3):1139–1164, 2007.
 - [20] Z. Harchaoui, F. Bach, and E. Moulines. Kernel change-point analysis. In *Advances in Neural Information Processing Systems (NIPS)*, pages 609–616, 2009.
 - [21] D. Hawkins and Q. Deng. A Nonparametric Change-Point Control Chart. *Journal of Quality Technology*, 42(2):165–173, 2010.
 - [22] N. Khan, S. McClean, S. Zhang, and C. Nugent. Optimal Parameter Exploration for Online Change-Point Detection in Activity Monitoring Using Genetic Algorithms. *Sensors*, 16(11), 2016.
 - [23] D. Kifer, S. Ben-david, and J. Gehrke. Detecting Change in Data Streams. *Proceedings of the 30th VLDB Conference*, pages 180–191, 2004.

- [24] A. Y. Kim, C. Marzban, D. Percival, and W. Stuetzle. Using labeled data to evaluate change detectors in a multivariate streaming environment. *Signal Processing*, 89(12):2529–2536, 2009.
- [25] Q. V. Le, T. Sarlós, and A. J. Smola. Fastfood — Approximating Kernel Expansions in Loglinear Time. In *International Conference on Machine Learning (ICML)*, volume 28, 2013.
- [26] S. Li, Y. Xie, H. Dai, and L. Song. Scan B-Statistic for Kernel Change-Point Detection. *arXiv:1507.01279*, pages 1–48, 2015.
- [27] Y. Li, K. Swersky, and R. Zemel. Generative Moment Matching Networks. *Proceedings of The 32nd International Conference on Machine Learning*, 37:1718–1727, 2015.
- [28] S. Liu, M. Yamada, N. Collier, and M. Sugiyama. Change-point detection in time-series data by relative density-ratio estimation. *Neural Networks*, 43:72–83, 2013.
- [29] C. A. Lowry and W. H. Woodall. A multivariate exponentially weighted moving average control chart. *Technometrics*, 34(1):46–53, 1992.
- [30] R. Malladi, G. P. Kalamangalam, and B. Aazhang. Online bayesian change point detection algorithms for segmentation of epileptic activity. In *Asilomar Conference on Signals, Systems and Computers*, pages 1833–1837, Nov 2013.
- [31] L. Peel and A. Clauset. Detecting change points in the large-scale structure of evolving networks. In *AAAI Conference on Artificial Intelligence*, pages 1–11, 2015.
- [32] A. Polunchenko and A. Tartakovsky. State-of-the-art in sequential change-point detection. *Methodology and computing in applied probability*, 14(3):649–684, 2012.
- [33] A. Rahimi and B. Recht. Random Features for Large Scale Kernel Machines. In *Advances in Neural Information Processing Systems (NIPS)*, 2007.
- [34] S. W. Roberts. Control Chart Tests Based on Geometric Moving Averages. *Technometrics*, 1(3):239–250, 1959.
- [35] A. Saade, F. Caltagirone, I. Carron, L. Daudet, A. Dremeau, S. Gigan, and F. Krzakala. Random projections through multiple optical scattering: Approximating Kernels at the speed of light. In *IEEE International Conference on Acoustic, Speech and Signal Processing (ICASSP)*, pages 6215–6219, 2016.
- [36] R. J. Serfling. *Approximation Theorems of Mathematical Statistics*, volume 37. John Wiley & Sons, Inc., 1980.
- [37] B. K. Sriperumbudur, A. Gretton, K. Fukumizu, B. Schölkopf, and G. R. Lanckriet. Hilbert space embeddings and metrics on probability measures. *The Journal of Machine Learning Research*, 11: 1517–1561, 2010.
- [38] M. Staudacher, S. Telser, A. Amann, H. Hinterhuber, and M. Ritsch-Marte. A new method for change-point detection developed for on-line analysis of the heart beat variability during sleep. *Physica A: Statistical Mechanics and its Applications*, 349(3):582 – 596, 2005.
- [39] D. J. Sutherland, J. B. Oliva, P. Barnabas, and J. Schneider. Linear-time Learning on Distributions with Approximate Kernel Embeddings. *arXiv:1509.07553*, 2015.
- [40] A. W. van der Vaart. *Asymptotic Statistics*. Cambridge University Press, 1998.
- [41] Y. Xie, J. Huang, and R. Willett. Change-point detection for high-dimensional time series with missing data. *IEEE Journal on Selected Topics in Signal Processing*, 7(1):12–27, 2013.
- [42] T. Yang, M. Mahdavi, R. Jin, J. Yi, and S. Hoi. Online Kernel Selection: Algorithms and Evaluations. *Aaai*, pages 1197–1203, 2012.
- [43] C. Zou and F. Tsung. Likelihood Ratio-Based Distribution-Free EWMA Control Charts. *Journal of Quality Technology*, 42(2):1–23, 2010.

Appendix

In this Appendix we collect the proofs of all the theoretical results of the paper and some additional results. The proofs themselves are in Sec. A. A statement about the mean time between false alarms of NEWMA can be found in Sec. B. Finally, Sec. C contains technical results used throughout this Appendix.

A Proofs of the theoretical results

In this section we collect the proofs of all the theoretical results of the paper. We start with some elementary computations that are used throughout the rest of the proofs.

Set $0 < \lambda < \Lambda < 1$. For any $i, t \geq 1$, define $\alpha_0 = (1 - \Lambda)^t$, $\beta_0 = (1 - \lambda)^t$,

$$\alpha_i = \Lambda(1 - \Lambda)^{t-i} \quad \text{and} \quad \beta_i = \lambda(1 - \lambda)^{t-i}.$$

Then, for any $1 \leq t_1 < t_2 \leq t$,

$$\sum_{i=0}^{t_1} \alpha_i = (1 - \Lambda)^{t-t_1}, \quad \sum_{i=0}^{t_1} \beta_i = (1 - \lambda)^{t-t_1}, \quad (6)$$

$$\sum_{i=t_1}^{t_2} \alpha_i = (1 - \Lambda)^{t-t_2} - (1 - \Lambda)^{t-t_1+1}, \quad \sum_{i=t_1}^{t_2} \beta_i = (1 - \lambda)^{t-t_2} - (1 - \lambda)^{t-t_1+1}, \quad (7)$$

$$\text{and} \quad \sum_{i=1}^t \alpha_i^{r_1} \beta_i^{r_2} = \frac{\Lambda^{r_1} \lambda^{r_2}}{1 - A} (1 - A^t), \quad \text{with} \quad A = (1 - \Lambda)^{r_1} (1 - \lambda)^{r_2}. \quad (8)$$

A.1 Proof of Prop. 1

Recall that we defined

$$B = \left\lceil \frac{\log(\Lambda/\lambda)}{\log((1-\lambda)/(1-\Lambda))} \right\rceil.$$

Let $t > B \geq 1$. By construction of definition of \mathbf{z}_t and \mathbf{z}'_t and by definition α_i, β_i , we have

$$\begin{cases} \mathbf{z}_t &= \alpha_0 \mathbf{z}_0 + \sum_{i=1}^t \alpha_i \Psi(x_i) \\ \mathbf{z}'_t &= \beta_0 \mathbf{z}_0 + \sum_{i=1}^t \beta_i \Psi(x_i). \end{cases}$$

A straightforward computation yields that $t - B$ is the ‘‘shifting’’ point for the weight coefficients. Namely, for $i = 1, \dots, t - B$, we have $\alpha_i \geq \beta_i$, and for $i = t - B + 1, \dots, t$, we have $\beta_i \geq \alpha_i$. According to Eq. (6) and Eq. (7), $\sum_{i=0}^{t-B} (\alpha_i - \beta_i) = \sum_{i=t-B+1}^t (\beta_i - \alpha_i) = C$, where $C = (1 - \lambda)^B - (1 - \Lambda)^B$. Hence, if we define $a_i \stackrel{\text{def.}}{=} (\alpha_i - \beta_i)/C$ for $i = 0, \dots, t - B$ and $b_i \stackrel{\text{def.}}{=} (\beta_i - \alpha_i)/C$ for $i = t - B + 1, \dots, t$, we have

$$\begin{aligned} \mathbf{z}_t - \mathbf{z}'_t &= \sum_{i=1}^t (\alpha_i - \beta_i) \Psi(x_i) + (\alpha_0 - \beta_0) \mathbf{z}_0 \\ &= \sum_{i=t-B+1}^t (\alpha_i - \beta_i) \Psi(x_i) - \left(\sum_{i=1}^{t-B} (\beta_i - \alpha_i) \Psi(x_i) + (\beta_0 - \alpha_0) \mathbf{z}_0 \right) \\ \mathbf{z}_t - \mathbf{z}'_t &= C \cdot \left(\sum_{i=t-B+1}^t a_i \Psi(x_i) - \left(b_0 \mathbf{z}_0 + \sum_{i=1}^{t-B} b_i \Psi(x_i) \right) \right). \end{aligned}$$

□

A.2 Proof of Prop. 2

Prop. 2 is a direct consequence from the following, more general result.

Lemma 6 (Concentration of the detection statistic). *Suppose that $M = \sup_{x \in \mathbb{R}^d} \|\Psi(x)\| < +\infty$. At time t , assume that the last B_1 samples are drawn according to π' , and that the B_2 samples that came immediately before were drawn from π (samples before that can be anything), and that $B_1 + B_2 \geq B$ for simplicity. Then, with probability at least $1 - \rho$ on the samples, we have*

$$\left| \|\mathbf{z}_t - \mathbf{z}'_t\| - Cd_{\Psi}(\pi', \pi) \right| \leq E_{\text{conc.}} + E_{\text{init.}} + E_{\text{assum.}}, \quad (9)$$

where

$$E_{\text{conc.}} = 2\sqrt{2}M \left(1 + \sqrt{\log \frac{2}{\rho}}\right) \sqrt{\varphi(\Lambda, \Lambda) + \varphi(\lambda, \lambda) - 2\varphi(\Lambda, \lambda)} \lesssim \varepsilon_1,$$

$$\text{with } \varphi(\Lambda, \lambda) = \frac{\Lambda\lambda(1-(1-\lambda)^t(1-\Lambda)^t)}{\Lambda+\lambda-\Lambda\lambda},$$

$$E_{\text{init.}} = ((1-\lambda)^t - (1-\Lambda)^t) \|\mathbf{z}_0 - \mathbb{E}_{\pi}\Psi(x)\| = \varepsilon_2,$$

$$\begin{aligned} E_{\text{assum.}} &= 2M \left((1-\lambda)^{B_1+B_2} - (1-\lambda)^t - [(1-\Lambda)^{B_1+B_2} - (1-\Lambda)^t] \right. \\ &\quad \left. + \left| (1-\lambda)^{\min(B, B_1)} - (1-\lambda)^{\max(B, B_1)} - \left[(1-\Lambda)^{\min(B, B_1)} - (1-\Lambda)^{\max(B, B_1)} \right] \right| \right) \\ &\lesssim M \min(1, |D_1 - 1| + |D_2 - 1|). \end{aligned}$$

where $D_1 = \frac{B_1}{B}$ and $D_2 = \frac{B_2}{t-B}$.

Proof. We have seen that, ideally, the last B samples are drawn from π' , and all the samples that came before are drawn from π . Let us call I the time interval of samples that are not drawn from the “correct” distribution:

$$I \stackrel{\text{def.}}{=} \llbracket 1, t - B_1 - B_2 \rrbracket \cup \llbracket t - \max(B, B_1) + 1, t - \min(B_1, B) \rrbracket.$$

Let us introduce “ghost samples” y_1, \dots, y_t drawn from the “correct” distributions, *i.e.* such that $y_1, \dots, y_{t-B} \stackrel{i.i.d.}{\sim} \pi$, $y_{t-B+1}, \dots, y_t \stackrel{i.i.d.}{\sim} \pi'$, and such that $y_i = x_i$ for $i \notin I$. The idea of the proof is to introduce the analogous of $\|\mathbf{z}_t - \mathbf{z}'_t\|$ for the ghost samples in the left-hand side of Eq. (9), to use the triangle inequality, and then to bound the resulting error terms. Thus, with the help of Prop. 1, we first write

$$\begin{aligned} \left| \|\mathbf{z}_t - \mathbf{z}'_t\| - Cd_{\Psi}(\pi, \pi') \right| &= \left| \left\| (\alpha_0 - \beta_0)\mathbf{z}_0 + \sum_{i=1}^t (\alpha_i - \beta_i)\Psi(x_i) \right\| - C \|\mathbb{E}_{\pi}\Psi(y) - \mathbb{E}_{\pi'}\Psi(y)\| \right| \\ &\leq \left| \left\| (\alpha_0 - \beta_0)\mathbf{z}_0 + \sum_{i=1}^t (\alpha_i - \beta_i)\Psi(y_i) \right\| - C \|\mathbb{E}_{\pi}\Psi(y) - \mathbb{E}_{\pi'}\Psi(y)\| \right| \\ &\quad + \left| \left\| (\alpha_0 - \beta_0)\mathbf{z}_0 + \sum_{i=1}^t (\alpha_i - \beta_i)\Psi(y_i) \right\| - \left\| (\alpha_0 - \beta_0)\mathbf{z}_0 + \sum_{i=1}^t (\alpha_i - \beta_i)\Psi(x_i) \right\| \right| \\ &\stackrel{\text{def.}}{=} \text{(I)} + \text{(II)}. \end{aligned}$$

since $|x - y| \leq |z - x| + |z - y|$.

We first show that (II) is upper bounded by $E_{\text{assum.}}$. Since $y_i = x_i$ for any $i \notin I$,

$$\text{(II)} \leq 2M \sum_{i \in I} |\alpha_i - \beta_i|.$$

By definition of the integer interval I ,

$$\begin{aligned} \sum_{i \in I} |\alpha_i - \beta_i| &= \sum_{i=1}^{t-B_1-B_2} |\alpha_i - \beta_i| + \sum_{i=t-\max(B, B_1)+1}^{t-\min(B, B_1)} |\alpha_i - \beta_i| \\ &= \left| \sum_{i=1}^{t-B_1-B_2} (\beta_i - \alpha_i) \right| + \left| \sum_{i=t-\max(B, B_1)+1}^{t-\min(B, B_1)} (\alpha_i - \beta_i) \right|, \end{aligned}$$

since $\alpha_i - \beta_i$ has constant sign in the considered intervals. Using Eq. (6) and (7), we obtain the desired expression for $E_{\text{assum.}}$. For simplicity, we then show that $E_{\text{assum.}}$ is roughly bounded by $M \min(1, |D_1 - 1| + |D_2 - 1|)$ up to a multiplicative constant. First, it is at least bounded by $4M$, and then, we have for instance

$$\begin{aligned} (1 - \lambda)^{B_1+B_2} - (1 - \lambda)^t &= (1 - \lambda)^{B_1+B_2} \left(1 - (1 - \lambda)^{t-B_1-B_2}\right) \\ &= (1 - \lambda)^{D_2 t + (D_1 - D_2)B} \left(1 - (1 - \lambda)^{(1-D_2)t + (D_2 - D_1)B}\right) \\ &\leq \left[(1 - \lambda)^{D_2 t + (D_1 - D_2)B} (t + B) \log \frac{1}{1 - \lambda} \right] \cdot (|D_2 - 1| + |D_1 - D_2|), \end{aligned}$$

and it is easy to show that the left multiplicative term is bounded. We proceed similarly for the other terms in $E_{\text{assum.}}$.

We now prove that (I) is upper bounded by $E_{\text{init.}} + E_{\text{conc.}}$. By the triangle inequality and the definition of a_i and b_i ,

$$\begin{aligned} \text{(I)} &\leq \left\| (\beta_0 - \alpha_0) \mathbf{z}_0 + \sum_{i=1}^{t-B} (\beta_i - \alpha_i) \Psi(y_i) - C \mathbb{E}_\pi \Psi(y) - \left(\sum_{i=t-B+1}^t (\alpha_i - \beta_i) \Psi(y_i) - C \mathbb{E}_{\pi'} \Psi(y) \right) \right\| \\ &\leq C b_0 \|\mathbf{z}_0 - \mathbb{E}_\pi \Psi(y)\| + C \left\| \sum_{i=1}^{t-B} b_i (\Psi(y_i) - \mathbb{E}_\pi \Psi(y)) \right\| + C \left\| \sum_{i=t-B+1}^t a_i (\Psi(y_i) - \mathbb{E}_{\pi'} \Psi(y)) \right\| \end{aligned}$$

since $\sum_{i=0}^{t-B} (\beta_i - \alpha_i) = \sum_{i=t-B+1}^t (\alpha_i - \beta_i) = C$.

We now apply McDiarmid's inequality (Lemma 11) to bound the right-hand side of the last display with high probability. Define $\Delta : (\mathbb{R}^d)^{t-B} \rightarrow \mathbb{R}$ by

$$\Delta(y_1, \dots, y_{t-B}) = \left\| \sum_{i=1}^{t-B} b_i (\Psi(y_i) - \mathbb{E}_\pi \Psi(y)) \right\|.$$

This function satisfies the bounded difference property, that is,

$$|\Delta(y_1, \dots, y_i, \dots, y_{t-B}) - \Delta(y_1, \dots, y'_i, \dots, y_{t-B})| \leq 2M a_i.$$

We then apply Lemma 11 with $f = \Delta$ and $c_i = 2M a_i$ to obtain

$$\mathbb{P}(\Delta \geq \mathbb{E}\Delta + \varepsilon) \leq \exp\left(-\frac{\varepsilon^2}{4M^2 \left(\sum_{i=1}^{t-B} b_i^2\right)}\right).$$

We now bound $\mathbb{E}\Delta$ by a symmetrization argument. Let us introduce the random variables y'_i that have the same law as the y_i and are independent from the y_i , and the σ_i , Rademacher random variables independent from both y_i and y'_i . We write

$$\begin{aligned} \mathbb{E} \left\| \sum_{i=1}^{t-B} b_i (\Psi(y_i) - \mathbb{E}\Psi(y)) \right\| &= \mathbb{E}_{y, y'} \left\| \sum_{i=1}^{t-B} b_i (\Psi(y_i) - \Psi(y'_i)) \right\| \\ &= \mathbb{E}_{y, y', \sigma} \left\| \sum_{i=1}^{t-B} b_i \sigma_i (\Psi(y_i) - \Psi(y'_i)) \right\| \leq 2 \mathbb{E}_y \mathbb{E}_\sigma \left\| \sum_{i=1}^{t-B} b_i \sigma_i \Psi(y_i) \right\| \\ &= 2 \sqrt{\mathbb{E}_y \mathbb{E}_\sigma \sum_{i, j=1}^{t-B} b_i b_j \sigma_i \sigma_j \langle \Psi(y_i), \Psi(y_j) \rangle_{\mathcal{H}}} \leq 2M \sqrt{\sum_{i=1}^{t-B} b_i^2} \end{aligned}$$

By applying the same reasoning to $\Delta' \stackrel{\text{def.}}{=} \left\| \sum_{i=t-B+1}^t a_i (\Psi(y_i) - \mathbb{E}_{\pi'} \Psi(y)) \right\|$ and a union bound, we obtain that, with probability at least $1 - \rho$,

$$\text{(I)} \leq E_{\text{init.}} + 2MC \left(1 + \sqrt{\log \frac{2}{\rho}}\right) \left(\sqrt{\sum_{i=t-B+1}^t a_i^2} + \sqrt{\sum_{i=1}^{t-B} b_i^2} \right).$$

Since

$$\begin{aligned} \sqrt{\sum_{i=t-B+1}^t a_i^2} + \sqrt{\sum_{i=1}^{t-B} b_i^2} &\leq \sqrt{2} \sqrt{\sum_{i=t-B+1}^t a_i^2 + \sum_{i=1}^{t-B} b_i^2} \\ &= \frac{\sqrt{2}}{C} \sqrt{\sum_{i=1}^t (\alpha_i^2 + \beta_i^2 - 2\alpha_i\beta_i)}, \end{aligned}$$

we recover the expression of $E_{\text{conc.}}$ with the help of Eq. (8). Therefore, we showed that, with probability at least $1 - \rho$,

$$\| \mathbf{z}_t - \mathbf{z}'_t \| - C d_{\Psi}(\pi, \pi') \leq E_{\text{conc.}} + E_{\text{init.}} + E_{\text{assum.}} .$$

□

A.3 Proof of Prop. 4

The proof is a combination of Prop. 2 and the following lemma, which is a consequence of Hoeffding's inequality.

Lemma 7 (Concentration of d_{Ψ}). *Define Ψ as (3) and let $\rho \in (0, 1)$. For any distributions π, π' , with probability at least $1 - \rho$ on the ω_j 's, we have*

$$d_{\Psi}(\pi, \pi')^2 \geq \text{MMD}(\pi, \pi')^2 - \frac{2\sqrt{2}M^2}{\sqrt{m}} \sqrt{\log \frac{1}{\rho}} .$$

Proof. One can show [37] that the MMD can also be expressed as

$$\text{MMD}(\pi, \pi')^2 = \int |\phi_{\omega}(\pi) - \phi_{\omega}(\pi')|^2 d\Gamma(\omega) .$$

where $\phi_{\omega}(\pi) \stackrel{\text{def.}}{=} \int \phi_{\omega}(x) d\pi(x)$. By the definition of $\Psi(x) = \frac{1}{\sqrt{m}} (\varphi_{\omega_j}(x))_{j=1}^m$,

$$d_{\Psi}(\pi, \pi')^2 = \frac{1}{m} \sum_{j=1}^m |\phi_{\omega_j}(\pi) - \phi_{\omega_j}(\pi')|^2 .$$

Since $\sup_{x, \omega} |\phi_{\omega}(x)| \leq M$, we deduce that $|\phi_{\omega_j}(\pi) - \phi_{\omega_j}(\pi')|^2 \leq 4M^2$ we can apply Hoeffding's inequality (Lemma 10) to d_{Ψ} . Thus, with probability $1 - \rho$, it holds that

$$\text{MMD}(\pi, \pi')^2 - d_{\Psi}(\pi, \pi')^2 \leq \frac{2\sqrt{2}M^2}{\sqrt{m}} \sqrt{\log \frac{1}{\rho}} .$$

□

A.4 Proof of Th. 5

Our proof follows closely [36], Sec. 5.5.2. with some modifications.

In the following, we let $\lambda \rightarrow 0$ with $\Lambda = c\lambda$ and $t \geq \frac{2}{\lambda} \log(1/\lambda)$ (which goes to $+\infty$ when λ goes to 0), such that $(1 - \lambda)^t = \mathcal{O}(\lambda^2)$. At time t , we denote $\gamma_i = \beta_i - \alpha_i$, with α and β defined as in the proof of Prop. 1. Note that α and β also depend on λ , and that by Eq. (8) we have

$$\frac{1}{\lambda} \sum_{i=1}^t \gamma_i^2 \xrightarrow{\lambda \rightarrow 0} G \stackrel{\text{def.}}{=} \frac{(1-c)^2}{2(1+c)}, \quad (10)$$

and $\sum_{i=1}^t \gamma_i^q = \mathcal{O}(\lambda^{q-1})$.

Define $\mu \stackrel{\text{def.}}{=} \mathbb{E}\Psi(x)$. At time t we have

$$\begin{aligned}
\frac{1}{\lambda} \|\mathbf{z}_t - \mathbf{z}'_t\|^2 &= \frac{1}{\lambda} \left\| \gamma_0 \mathbf{z}_0 + \sum_{i=1}^t \gamma_i \Psi(x_i) \right\|^2 \\
&= \frac{1}{\lambda} \left\| \gamma_0 (\mathbf{z}_0 - \mu) + \sum_{i=1}^t \gamma_i (\Psi(x_i) - \mu) \right\|^2 \quad \text{since } \sum_{i=0}^t \gamma_i = 0 \\
&= \frac{1}{\lambda} \sum_{i,j=1}^t \gamma_i \gamma_j K(x_i, x_j) + \frac{2}{\lambda} \gamma_0 \sum_{i=1}^t \gamma_i \langle \mathbf{z}_0 - \mu, \Psi(x_i) - \mu \rangle_{\mathcal{H}} + \frac{1}{\lambda} \gamma_0^2 \|\mathbf{z}_0 - \mu\|^2,
\end{aligned} \tag{11}$$

where K is a positive semi-definite kernel on \mathcal{H} defined by $K(x, x') = \langle \Psi(x) - \mu, \Psi(x') - \mu \rangle_{\mathcal{H}}$.

The last term of Eq. (11) is deterministic and goes to 0 with λ since $\gamma_0^2 = \mathcal{O}(\lambda^4)$. Let us now prove that the second term converges in probability to 0. By Cauchy-Schwarz's and Jensen's inequalities we have

$$\begin{aligned}
\mathbb{E} \langle \mathbf{z}_0 - \mu, \Psi(x_i) - \mu \rangle_{\mathcal{H}} \langle \mathbf{z}_0 - \mu, \Psi(x_j) - \mu \rangle_{\mathcal{H}} &\leq \|\mathbf{z}_0 - \mu\|^2 \mathbb{E} \sqrt{K(x_i, x_i) K(x_j, x_j)} \\
&\leq \|\mathbf{z}_0 - \mu\|^2 \mathbb{E} K(x, x) < \infty, \text{ and} \\
\frac{1}{\lambda} \gamma_0 &= \mathcal{O}(\lambda) \xrightarrow{\lambda \rightarrow 0} 0
\end{aligned}$$

Hence $\frac{2}{\lambda} \gamma_0 \sum_{i=1}^t \gamma_i \langle \mathbf{z}_0 - \mu, \Psi(x_i) - \mu \rangle_{\mathcal{H}}$ has a second order moment that converges to 0, and by Markov's inequality it converges in probability to 0.

Let us now prove that the first term in Eq. (11) converges in law, and conclude with Slutsky's Lemma (Lemma 13). We start by using Mercer's theorem on K , within the ambient space $L^2(\pi)$: we write

$$K(x, x') = \sum_{\ell \geq 1} \xi_\ell \psi_\ell(x) \psi_\ell(x'),$$

with $\xi_\ell \geq 0$ and $\langle \psi_\ell, \psi_{\ell'} \rangle_{L^2(\pi)} = 1_{\ell=\ell'}$, such that $\langle K(x, \cdot), \psi_\ell \rangle_{L^2(\pi)} = \xi_\ell \psi_\ell(x)$. Note that, since $\mathbb{E}_x K(x, x') = 0$, for any $\xi_\ell \neq 0$ we have $\mathbb{E} \psi_\ell(x) = \frac{1}{\xi_\ell} \langle \mathbb{E} K(x, \cdot), \psi_\ell \rangle_{L^2(\pi)} = 0$. Finally, we have $\sum_{\ell \geq 1} \xi_\ell^2 \mathbb{E} \psi_\ell^4(x) \leq \mathbb{E} K^2(x, x) < \infty$ since $\mathbb{E} \|\Psi(x)\|^4 < +\infty$.

Our goal is to show that $T_\lambda \stackrel{\text{def.}}{=} \frac{1}{\lambda} \sum_{i,j=1}^t \gamma_i \gamma_j K(x_i, x_j)$ converges in law to $Y = G \sum_{\ell \geq 1} \xi_\ell W_\ell^2$ where W_ℓ are independent centered normal variable. We are going to use the characteristic function method, *i.e.*, we are going to prove that:

$$\forall u \in \mathbb{R}, \quad \mathbb{E} e^{iuT_\lambda} \xrightarrow{\lambda \rightarrow 0} \mathbb{E} e^{iuY}.$$

Fix any $u \in \mathbb{R}$ and $\varepsilon > 0$. Our goal is to prove that, for λ sufficiently small, we have $|\mathbb{E} e^{iuT_\lambda} - \mathbb{E} e^{iuY}| \leq \varepsilon$. We decompose the bound in three parts.

Step 1. For an integer $k \geq 0$, define $T_\lambda^{(k)} = \frac{1}{\lambda} \sum_{i,j=1}^t \gamma_i \gamma_j \left[\sum_{\ell=1}^k \xi_\ell \psi_\ell(x_i) \psi_\ell(x_j) \right]$. We are first going to approach $\mathbb{E} e^{iuT_\lambda}$ by $\mathbb{E} e^{iuT_\lambda^{(k)}}$ for k sufficiently big. We write

$$\left| \mathbb{E} e^{iuT_\lambda} - \mathbb{E} e^{iuT_\lambda^{(k)}} \right| \leq \mathbb{E} \left| e^{iuT_\lambda} - e^{iuT_\lambda^{(k)}} \right| \leq |u| \mathbb{E} |T_\lambda - T_\lambda^{(k)}| \leq |u| \sqrt{\mathbb{E} (T_\lambda - T_\lambda^{(k)})^2}.$$

Denote $f_k(x, x') = K(x, x') - \sum_{\ell=1}^k \xi_\ell \psi_\ell(x) \psi_\ell(x') = \sum_{\ell \geq k+1} \xi_\ell \psi_\ell(x) \psi_\ell(x')$, such that $T_\lambda - T_\lambda^{(k)} = \frac{1}{\lambda} \sum_{i,j=1}^t \gamma_i \gamma_j f_k(x_i, x_j)$. We have $\mathbb{E} [f_k(x_1, x'_1) f_k(x_2, x'_2)] \neq 0$ if and only if both $x_1 = x_2$ and $x'_1 = x'_2$ (or permuted since f_k is symmetric), and we have

$$\begin{aligned}
\mathbb{E}_{x,x'} f_k(x, x')^2 &= \sum_{\ell \geq k+1} \xi_\ell^2 (\mathbb{E} \psi_\ell^2(x))^2 = \sum_{\ell \geq k+1} \xi_\ell^2 \\
\mathbb{E} f_k(x, x)^2 &= \sum_{\ell \geq k+1} \xi_\ell^2 \mathbb{E} \psi_\ell^4(x),
\end{aligned}$$

where the last expression is summable since $\mathbb{E}K^2(x, x) < \infty$. Then we have

$$\begin{aligned} \mathbb{E} \left(T_\lambda - T_\lambda^{(k)} \right)^2 &= \frac{1}{\lambda^2} \mathbb{E} \left[\sum_{i_1, j_1=1}^t \sum_{i_2, j_2=1}^t \gamma_{i_1} \gamma_{j_1} \gamma_{i_2} \gamma_{j_2} f_k(x_{i_1}, x_{j_1}) f_k(x_{i_2}, x_{j_2}) \right] \\ &\leq \frac{2}{\lambda^2} \mathbb{E} \left[\sum_{i, j=1}^t \gamma_i^2 \gamma_j^2 f_k(x_i, x_j)^2 \right] \\ &\leq 2 \left(\frac{1}{\lambda} \sum_{i=1}^t \gamma_i^2 \right)^2 \max(\mathbb{E}_{x, x'} f_k^2(x, x'), \mathbb{E} f_k^2(x, x)) \leq C \left(\sum_{\ell \geq k+1} \xi_\ell^2 \max(1, \mathbb{E} \psi_\ell^4(x)) \right), \end{aligned}$$

for some constant C , since $\sum_{i=1}^t \gamma_i^2 = \mathcal{O}(\lambda)$. Hence for k sufficiently big we have:

$$\forall \lambda \in (0, 1), \left| \mathbb{E} e^{iuT_\lambda} - \mathbb{E} e^{iuT_\lambda^{(k)}} \right| \leq \frac{\varepsilon}{3}. \quad (12)$$

Step 2. Let us now temporarily consider a fixed k , and prove that $T_\lambda^{(k)}$ converges in law to $Y^{(k)} = B \sum_{\ell=1}^k \xi_\ell W_\ell^2$. We write

$$T_\lambda^{(k)} = \frac{1}{\lambda} \sum_{i, j=1}^t \gamma_i \gamma_j \left[\sum_{\ell=1}^k \xi_\ell \psi_\ell(x_i) \psi_\ell(x_j) \right] = \sum_{\ell=1}^k \xi_\ell \left(\frac{1}{\sqrt{\lambda}} \sum_{i=1}^t \gamma_i \psi_\ell(x_i) \right)^2.$$

We now use Lindeberg's theorem (Th. 12) on the random vectors

$$X^{(i, t)} = \left(\frac{1}{\sqrt{\lambda}} \gamma_i \psi_\ell(x_i) \right)_{\ell=1}^k.$$

They are centered and their covariance is such that

$$\sum_{i=1}^t \text{Cov}(X^{(i, t)}) = \left(\frac{1}{\lambda} \sum_{i=1}^t \gamma_i^2 \right) \text{Id} \xrightarrow{\lambda \rightarrow 0} B \cdot \text{Id}.$$

We now check Lindeberg's condition (19). By Cauchy-Schwartz and Markov's inequality, for all $\delta > 0$ we have

$$\begin{aligned} \mathbb{E} \left[\left\| X^{(i, t)} \right\|^2 \mathbf{1}_{\{\|X^{(i, t)}\| \geq \delta\}} \right] &\leq \sqrt{\mathbb{E} \|X^{(i, t)}\|^4} \cdot \mathbb{P} \left[\left\| X^{(i, t)} \right\| \geq \delta \right] \\ &\leq \sqrt{\mathbb{E} \|X^{(i, t)}\|^4} \cdot \delta^{-2} \mathbb{E} \|X^{(i, t)}\|^2 \leq C \delta^{-2} \frac{\gamma_i^4}{\lambda^2}, \end{aligned}$$

where C is a constant, since $\psi_\ell(x)$ has finite second and fourth order moment. Using the fact that $\sum_{i=1}^t \frac{\gamma_i^4}{\lambda^2} = \mathcal{O}(\lambda)$, Lindeberg's condition is satisfied. Hence, applying theorem 12, $\sum_{i=1}^t X^{(i, t)}$ converges in law to $\mathcal{N}(0, G \cdot \text{Id})$, and $T_\lambda^{(k)}$ converges in law to $Y^{(k)}$. Hence for a sufficiently small λ

$$\left| \mathbb{E} e^{iuT_\lambda^{(k)}} - \mathbb{E} e^{iuY^{(k)}} \right| \leq \frac{\varepsilon}{3}. \quad (13)$$

Step 3. Finally, similar to Step 1 we have

$$\begin{aligned} \left| \mathbb{E} e^{iuY^{(k)}} - \mathbb{E} e^{iuY} \right| &\leq \mathbb{E} \left| e^{iuY^{(k)}} - e^{iuY} \right| \leq |u| \mathbb{E} |Y^{(k)} - Y| \leq |u| \sqrt{\mathbb{E} (Y^{(k)} - Y)^2} \\ &\leq |u| \left(\sum_{\ell \geq k+1} \xi_\ell \right)^2 \max(1, \mathbb{E} W^4) \quad \text{where } W \sim \mathcal{N}(0, 1), \end{aligned}$$

and therefore for a sufficiently big k

$$\left| \mathbb{E} e^{iuY^{(k)}} - \mathbb{E} e^{iuY} \right| \leq \frac{\varepsilon}{3}. \quad (14)$$

To conclude, we fix k large enough such that Eq. (12) and (14) are satisfied, then λ small enough and Eq. (13) is satisfied, which concludes the proof. \square

B Mean time between false alarm

Consider an online change-point detection algorithm that produces a statistic S_t that must not exceed a threshold τ . The mean time between false alarms, also called Average Run Length (ARL) under control, is the expected runtime of the algorithm when no change occurs. Assuming all samples x_t are drawn *i.i.d.* from a distribution π , recall that we define it as

$$\bar{T} = \mathbb{E}[\inf \{t \mid S_t \geq \tau\}]. \quad (15)$$

In the case of NEWMA, we have $S_t = \|\mathbf{z}_t - \mathbf{z}'_t\|$. In this section, we derive a more tractable expression for \bar{T} .

Our proof strategy relies on the observation that $(\mathbf{z}_t, \mathbf{z}'_t)$ is a Markov chain in \mathcal{H}^2 , and thus it is possible to apply a method similar to [13] for classical EWMA, with non-trivial modifications. We show that their approach can be adapted to NEWMA when $\mathcal{H} \stackrel{\text{def.}}{=} \mathbb{R}^m$ is finite-dimensional (that is, $\Psi : \mathbb{R}^d \rightarrow \mathbb{R}^m$). We consider $\mathbf{v}_t \stackrel{\text{def.}}{=} (\mathbf{z}_t, \mathbf{z}'_t)$ as the Markov chain of interest. Intuitively, we must handle several key points for NEWMA:

- *Multidimensionality*: we replace unidimensional grids by ε -coverings in \mathbb{R}^m .
- *Stopping condition*: the stopping condition for NEWMA involves both components \mathbf{z}_t and \mathbf{z}'_t of \mathbf{v}_t . We define the set $V_\tau \subset \mathcal{H}^2$ as the domain in which the algorithm continues:

$$V_\tau \stackrel{\text{def.}}{=} \{\mathbf{v} = (\mathbf{z}, \mathbf{z}') \mid \|\mathbf{z} - \mathbf{z}'\| < \tau\}. \quad (16)$$

- *Boundedness*: finally, here we do not assume that Ψ is bounded like in Prop. 2 for instance. As a consequence, neither \mathbf{z}_t nor \mathbf{z}'_t is bounded during the run. Nevertheless, we will show that we can handle this fact by discretizing a compact domain *whose size grows simultaneously as the net becomes finer*, which is sufficient for the convergence properties of interest to us.

With these notations, when we run NEWMA and stop as soon as an alarm is raised, we produce a Markov chain $\mathbf{v}_t \in \mathcal{H}^2$ defined as: $\mathbf{v}_0 = (\mathbf{z}_0, \mathbf{z}_0)$, and

$$\mathbf{v}_t = \begin{cases} \begin{pmatrix} (1 - \Lambda)\mathbf{v}_{t-1,1} + \Lambda\Psi(x_t) \\ (1 - \lambda)\mathbf{v}_{t-1,2} + \lambda\Psi(x_t) \end{pmatrix} & \text{if } \mathbf{v}_{t-1} \in V_\tau, \\ \mathbf{v}_{t-1} & \text{otherwise.} \end{cases}$$

In other words, the chain is stationary as soon as an alarm is raised.

Coverings. Let us now define the discretization that we will use for our Markov chain-based strategy. Consider the space $\mathcal{H}^2 = \mathcal{H} \times \mathcal{H}$, equipped with the norm $\|(\mathbf{x}, \mathbf{x}')\| = \|\mathbf{x}\| + \|\mathbf{x}'\|$. For $\varepsilon > 0$, consider the ball of radius ε^{-1} in \mathcal{H}^2 , $\mathcal{B}_\varepsilon = \{\mathbf{v} \mid \|\mathbf{v}\| \leq 1/\varepsilon\}$, which is compact since \mathcal{H}^2 has finite dimension. Define $\mathcal{C}_\varepsilon = \{\mathbf{u}_1, \dots, \mathbf{u}_{N_\varepsilon}\} \subset \mathcal{B}_\varepsilon$ any ε -net of \mathcal{B}_ε (we will see that its choice does not matter) such that $\mathbf{u}_1 = (\mathbf{z}_0, \mathbf{z}_0)$, where N_ε is the ε -covering number of \mathcal{B}_ε . Without loss of generality, assume they are ordered such that $\mathbf{u}_1, \dots, \mathbf{u}_{M_\varepsilon} \in V_\tau$ and $\mathbf{u}_{M_\varepsilon+1}, \dots, \mathbf{u}_{N_\varepsilon} \in V_\tau^c$ for some M_ε . Denote $P_\varepsilon : \mathcal{H}^2 \rightarrow \mathcal{C}_\varepsilon$ the projection operator onto \mathcal{C}_ε (*i.e.*, that returns the \mathbf{u}_i closest to its input).

Define the following Markov chain $\mathbf{v}_t^\varepsilon \in \mathcal{C}_\varepsilon$: initialize $\mathbf{v}_0^\varepsilon = (\mathbf{z}_0, \mathbf{z}_0) = \mathbf{u}_1$, and

$$\mathbf{v}_t^\varepsilon = \begin{cases} P_\varepsilon \left(\begin{pmatrix} (1 - \Lambda)\mathbf{v}_{t-1,1}^\varepsilon + \Lambda\Psi(x_t) \\ (1 - \lambda)\mathbf{v}_{t-1,2}^\varepsilon + \lambda\Psi(x_t) \end{pmatrix} \right) & \text{if } \mathbf{v}_{t-1}^\varepsilon \in V_\tau, \\ \mathbf{v}_{t-1}^\varepsilon & \text{otherwise.} \end{cases}$$

It is a *projected* and *bounded* version of the output of NEWMA, which is stationary as soon as it gets out of V_τ . A key observation is that the radius of \mathcal{B}_ε grows to $+\infty$ as $\varepsilon \rightarrow 0$.

For $1 \leq i, j \leq N_\varepsilon$, define $p_{ij} = \mathbb{P}(\mathbf{v}_{t+1}^\varepsilon = \mathbf{u}_j \mid \mathbf{v}_t^\varepsilon = \mathbf{u}_i)$ the transition probabilities of the markov chain \mathbf{v}_t^ε . Define $\mathbf{A} = [p_{ij}]_{1 \leq i, j \leq M_\varepsilon}$ that corresponds to the states $\mathbf{u}_i \in V_\tau$, all other states being absorbant, and $a_{ij}^{(\ell)}$ such that $\mathbf{A}^\ell = [a_{ij}^{(\ell)}]_{1 \leq i, j \leq M_\varepsilon}$.

Our result on the mean time between false alarms is the following.

Theorem 8 (Mean time between false alarms of NEWMA). Assume that π is such that $\Psi(x) \in \mathbb{R}^m$ has a density with respect to the Lebesgue measure when $x \sim \pi$. Then, the quantity $\gamma_\ell = \lim_{\varepsilon \rightarrow 0} \left(\sum_{j=1}^{M_\varepsilon} a_{ij}^{(\ell)} \right)$ does not depend on the choice of the nets \mathcal{C}_ε , and the mean time between false alarms of NEWMA is given by

$$\bar{T} = \mathbb{E} [\inf \{t \mid \|\mathbf{z}_t - \mathbf{z}'_t\| \geq \tau\}] = 1 + \sum_{\ell \geq 1} \gamma_\ell. \quad (17)$$

Our proof relies on the key lemma:

Lemma 9 (Almost sure convergence of \mathbf{v}_t^ε). For any fixed t , when ε goes to 0, \mathbf{v}_t^ε converges to \mathbf{v}_t almost surely.

Proof. Let us first note that, since by assumption $\Psi(x)$ has a density, is it easy to prove by recurrence on t that \mathbf{v}_t also has a density. Therefore, for all t , $\mathbb{P}(\mathbf{v}_t \in \partial V_\tau) = 0$ (it is trivial that the boundary of V_τ has zero Lebesgue measure), and by a countable union of zero-measure sets:

$$\mathbb{P}(\exists t \mid \mathbf{v}_t \in \partial V_\tau) = 0. \quad (18)$$

Since we want to prove an almost sure convergence, we explicitly denote by Ω the set of all events such that $\forall t, \mathbf{v}_t \notin \partial V_\tau$ (which has probability 1), and the events in Ω by ω . A draw of a r.v. X will be denoted by $X(\omega)$.

Fix any $t \geq 1$. Consider any $\omega \in \Omega$, corresponding to a draw of samples $x_\ell(\omega)$, $\ell = 1, \dots, t$. Remember that, by the definition of Ω , $\mathbf{v}_\ell(\omega) \notin \partial V_\tau$. Note that, when ε varies, the $\mathbf{v}_\ell^\varepsilon(\omega)$ change, but in a deterministic fashion. Our goal is to show that $\mathbf{v}_t^\varepsilon(\omega) \rightarrow \mathbf{v}_t(\omega)$ when $\varepsilon \rightarrow 0$.

We are going to show by induction that $\|\mathbf{v}_\ell^\varepsilon(\omega) - \mathbf{v}_\ell(\omega)\| \xrightarrow{\varepsilon \rightarrow 0} 0$ for all $\ell = 1, \dots, t$. Since $\mathbf{v}_0 = \mathbf{v}_0^\varepsilon$, it is obviously true for $\ell = 0$. Then, for any ℓ , suppose that $\|\mathbf{v}_{\ell-1}^\varepsilon(\omega) - \mathbf{v}_{\ell-1}(\omega)\| \xrightarrow{\varepsilon \rightarrow 0} 0$. By (18) we have either $\mathbf{v}_{\ell-1}(\omega) \in V_\tau$ or $\mathbf{v}_{\ell-1}(\omega) \in \overline{V_\tau}^c$ since it does not belong to the boundary. We study separately these two cases.

$\mathbf{v}_{\ell-1}(\omega)$ inside of V_τ . Since by inductive hypothesis $\|\mathbf{v}_{\ell-1}^\varepsilon(\omega) - \mathbf{v}_{\ell-1}(\omega)\| \xrightarrow{\varepsilon \rightarrow 0} 0$, and since V_τ is an open set of \mathbb{R}^{2m} , for all ε sufficiently small we have that $\mathbf{v}_{\ell-1}^\varepsilon(\omega) \in V_\tau$ and the Markov chain \mathbf{v}^ε is updated at step ℓ . Furthermore, since the radius of \mathcal{B}_ε goes to ∞ when $\varepsilon \rightarrow 0$, for all ε sufficiently small, $\mathbf{v}_\ell(\omega) \in \mathcal{B}_\varepsilon$, and $\|P_\varepsilon(\mathbf{v}_\ell(\omega)) - \mathbf{v}_\ell(\omega)\| \leq \varepsilon$. Hence, in that case,

$$\begin{aligned} \|\mathbf{v}_\ell^\varepsilon(\omega) - \mathbf{v}_\ell(\omega)\| &\leq \|\mathbf{v}_\ell^\varepsilon(\omega) - P_\varepsilon(\mathbf{v}_\ell(\omega))\| + \varepsilon \\ &\hspace{15em} \text{(triangle inequality)} \\ &= \left\| P_\varepsilon \left(\begin{pmatrix} (1-\Lambda)\mathbf{v}_{\ell-1,1}^\varepsilon(\omega) + \Lambda\Psi(x_\ell(\omega)) \\ (1-\lambda)\mathbf{v}_{\ell-1,2}^\varepsilon(\omega) + \lambda\Psi(x_\ell(\omega)) \end{pmatrix} \right) \right. \\ &\quad \left. - P_\varepsilon \left(\begin{pmatrix} (1-\Lambda)\mathbf{v}_{\ell-1,1}(\omega) + \Lambda\Psi(x_\ell(\omega)) \\ (1-\lambda)\mathbf{v}_{\ell-1,2}(\omega) + \lambda\Psi(x_\ell(\omega)) \end{pmatrix} \right) \right\| + \varepsilon \\ &\hspace{15em} \text{(definition of } \mathbf{v}_\ell \text{ and } \mathbf{v}_\ell^\varepsilon) \\ &\leq \left\| \begin{pmatrix} (1-\Lambda)\mathbf{v}_{\ell-1,1}^\varepsilon(\omega) + \Lambda\Psi(x_\ell(\omega)) \\ (1-\lambda)\mathbf{v}_{\ell-1,2}^\varepsilon(\omega) + \lambda\Psi(x_\ell(\omega)) \end{pmatrix} \right. \\ &\quad \left. - \begin{pmatrix} (1-\Lambda)\mathbf{v}_{\ell-1,1}(\omega) + \Lambda\Psi(x_\ell(\omega)) \\ (1-\lambda)\mathbf{v}_{\ell-1,2}(\omega) + \lambda\Psi(x_\ell(\omega)) \end{pmatrix} \right\| + \varepsilon \\ &\hspace{15em} \text{(projections are contracting)} \\ &\leq (1-\Lambda) \|\mathbf{v}_{\ell-1,1}^\varepsilon(\omega) - \mathbf{v}_{\ell-1,1}(\omega)\| + (1-\lambda) \|\mathbf{v}_{\ell-1,2}^\varepsilon(\omega) - \mathbf{v}_{\ell-1,2}(\omega)\| + \varepsilon \\ &\hspace{15em} \text{(definition of the norm)} \\ &\leq \|\mathbf{v}_{\ell-1}^\varepsilon(\omega) - \mathbf{v}_{\ell-1}(\omega)\| + \varepsilon. \end{aligned}$$

Therefore $\|\mathbf{v}_\ell^\varepsilon(\omega) - \mathbf{v}_\ell(\omega)\| \xrightarrow{\varepsilon \rightarrow 0} 0$.

$\mathbf{v}_{\ell-1}(\omega)$ **outside** $\overline{V_\tau}$. We have $\mathbf{v}_\ell(\omega) = \mathbf{v}_{\ell-1}(\omega)$ by definition of the Markov chain \mathbf{v}_t . Since $\overline{V_\tau}^c$ is an open set, by inductive hypothesis for all ε sufficiently small we have $\mathbf{v}_{\ell-1}^\varepsilon(\omega) \in \overline{V_\tau}^c$ and $\mathbf{v}_\ell^\varepsilon(\omega) = \mathbf{v}_{\ell-1}^\varepsilon(\omega)$, from which $\|\mathbf{v}_\ell^\varepsilon(\omega) - \mathbf{v}_\ell(\omega)\| = \|\mathbf{v}_{\ell-1}^\varepsilon(\omega) - \mathbf{v}_{\ell-1}(\omega)\| \xrightarrow{\varepsilon \rightarrow 0} 0$, which concludes the proof. \square

We can now turn to proving the theorem itself.

Proof of Th. 8. We start by a reformulation:

$$\begin{aligned} \overline{T} &= \mathbb{E}[\inf \{t \mid \|\mathbf{z}_t - \mathbf{z}'_t\| \geq \tau\}] = \mathbb{E}(\inf \{t \mid \mathbf{v}_t \notin V_\tau\}) \\ &= \sum_{\ell \geq 0} \mathbb{P}(\inf \{t \mid \mathbf{v}_t \notin V_\tau\} > \ell) = 1 + \sum_{\ell \geq 1} \mathbb{P}(\mathbf{v}_\ell \in V_\tau), \end{aligned}$$

since the first time \mathbf{v}_t exits V_τ is strictly greater than ℓ if, and only if, $\mathbf{v}_\ell \in V_\tau$.

Since almost sure convergence implies weak convergence, by Lemma 9, we have

$$\overline{T} = 1 + \sum_{\ell \geq 1} \lim_{\varepsilon \rightarrow 0} \mathbb{P}(\mathbf{v}_\ell^\varepsilon \in V_\tau).$$

Note that the convergence in ε is not necessarily uniform: in general, one cannot exchange the limit operator with the infinite sum in the last display.

To conclude the proof, we just have to compute $\mathbb{P}(\mathbf{v}_\ell^\varepsilon \in V_\tau)$. For $1 \leq i, j \leq N_\varepsilon$, recall that we defined the transition probabilities of the Markov chain \mathbf{v}_t^ε by

$$p_{ij} = \mathbb{P}(\mathbf{v}_{t+1}^\varepsilon = \mathbf{u}_j \mid \mathbf{v}_t^\varepsilon = \mathbf{u}_i).$$

The transition matrix of this Markov chain has the form:

$$\mathbf{P} = [p_{ij}]_{1 \leq i, j \leq N_\varepsilon} = \begin{bmatrix} \mathbf{A} & \mathbf{B} \\ \mathbf{0} & \text{Id} \end{bmatrix},$$

where $\mathbf{A} = [p_{ij}]_{1 \leq i, j \leq M_\varepsilon}$ corresponds to the states $\mathbf{u}_i \in V_\tau$. Then, if we define $a_{ij}^{(\ell)}$ such that $\mathbf{A}^\ell = [a_{ij}^{(\ell)}]_{1 \leq i, j \leq M_\varepsilon}$, it is possible to show by induction [13] that:

$$\begin{aligned} \mathbf{P}^\ell &= \begin{bmatrix} \mathbf{A}^\ell & \left(\sum_{i=0}^{\ell-1} \mathbf{A}^i\right) \mathbf{B} \\ \mathbf{0}_{(N_\varepsilon - M_\varepsilon) \times M_\varepsilon} & \text{Id}_{N_\varepsilon - M_\varepsilon} \end{bmatrix}, \text{ and therefore} \\ \mathbb{P}(\mathbf{v}_\ell^\varepsilon \in V_\tau) &= [1, 0, \dots, 0] \mathbf{P}^\ell \begin{pmatrix} \mathbf{1}_{M_\varepsilon} \\ \mathbf{0}_{N_\varepsilon - M_\varepsilon} \end{pmatrix} = [1, 0, \dots, 0] \mathbf{A}^\ell \mathbf{1}_{M_\varepsilon} = \sum_{j=1}^{M_\varepsilon} a_{1j}^{(\ell)}, \end{aligned}$$

which concludes the proof. \square

Application to the unidimensional case. We conclude this section by describing approximate closed-form expression for Th. 8 when $m = 1$ and the c.d.f. of $\Psi(x)$ is known.

Fix a small $\varepsilon > 0$ that we will use for our approximation, a grid $G \stackrel{\text{def.}}{=} \{a_1, \dots, a_N\} \subset [-1/\varepsilon, 1/\varepsilon]$ of ε -separated points (one can replace $1/\varepsilon$ by a smaller value to save some computation time at the expense of losing in accuracy), and $\mathcal{B}_\varepsilon = G \times G$. For any two states $\mathbf{u}_i = (a_i, b_i)$ and $\mathbf{u}_j = (a_j, b_j)$, both in V_τ , we have

$$\begin{aligned} p_{ij} &= \mathbb{P}(\mathbf{v}_t^\varepsilon = \mathbf{u}_j \mid \mathbf{v}_{t-1}^\varepsilon = \mathbf{u}_i) \\ &= \mathbb{P}((1 - \Lambda)a_i + \Lambda\Psi(x) \in [a_j \pm \varepsilon/2] \text{ and } (1 - \lambda)b_i + \lambda\Psi(x) \in [b_j \pm \varepsilon/2]) \\ &= \mathbb{P}(\Psi(x) \in [\ell, u]), \end{aligned} \quad \begin{array}{l} \text{(definition pf } p_{ij}) \\ \text{(definition of the detection statistic)} \end{array}$$

where we introduced

$$\begin{cases} \ell &= \max\left(\frac{1}{\Lambda}(a_j - (1 - \Lambda)a_i - \varepsilon/2), \frac{1}{\lambda}(b_j - (1 - \lambda)b_i - \varepsilon/2)\right), \\ u &= \min\left(\frac{1}{\Lambda}(a_j - (1 - \Lambda)a_i + \varepsilon/2), \frac{1}{\lambda}(b_j - (1 - \lambda)b_i + \varepsilon/2)\right). \end{cases}$$

Hence

$$p_{ij} = \begin{cases} \mathbb{P}(\Psi(x) \leq u) - \mathbb{P}(\Psi(x) \leq \ell) & \text{if } \ell < u \\ 0 & \text{otherwise.} \end{cases}$$

Using this expression, one can compute the matrix $\mathbf{A} = [p_{ij}]$.

Then, since we are reasoning at a fixed ε , we can use a Von Neumann series on \mathbf{A} in Eq. (17), that is, $\sum_{\ell \geq 0} \mathbf{A}^\ell = (\text{Id} - \mathbf{A})^{-1}$. Note that one cannot exchange the limit “ $\lim_{\varepsilon \rightarrow 0}$ ” and the infinite sum “ $\sum_{\ell \geq 1}$ ” in Eq. (17) since the convergence in ε is not uniform. Nevertheless, for the sake of approximate numerical computations with a fixed ε , we write

$$\bar{T} \approx 1 + \sum_{\ell \geq 1} (\mathbf{e}_1^\top \mathbf{A}^\ell \mathbf{1}) = \mathbf{e}_1^\top (\text{Id} - \mathbf{A})^{-1} \mathbf{1}$$

where $\mathbf{1} = [1, \dots, 1]^\top$ and $\mathbf{e}_1 = [1, 0, \dots, 0]^\top$.

We illustrate this principle in the paper (see the right panel of Fig. 2) with a Gaussian distribution, and find the above approximation to be quite accurate, even for moderate values of ε .

C Third-party technical results

We start the Appendix by recalling some technical results that will be used in the proofs.

Lemma 10 (Hoeffding’s inequality ([7], Th. 2.8)). *Let X_i be independent, bounded random variables such that $X_i \in [a_i, b_i]$ a.s. Then, for any $t > 0$,*

$$\mathbb{P}\left(\frac{1}{n} \sum_{i=1}^n X_i - \mathbb{E}\left(\frac{1}{n} \sum_{i=1}^n X_i\right) \geq t\right) \leq \exp\left(-\frac{2n^2 t^2}{\sum_{i=1}^n (a_i - b_i)^2}\right).$$

Lemma 11 (McDiarmid’s inequality ([7], Th. 6.2)). *Let $f : E^n \rightarrow \mathbb{R}$ be a measurable function that satisfies the bounded difference property, that is, there exist positive numbers c_1, \dots, c_n such that*

$$\sup_{x_1, \dots, x_n, x'_i \in E} |f(x_1, \dots, x_i, \dots, x_n) - f(x_1, \dots, x'_i, \dots, x_n)| \leq c_i.$$

Let X_1, \dots, X_n be independent random variables with values in E and set $Z = f(X_1, \dots, X_n)$. Then

$$\mathbb{P}(Z - \mathbb{E}Z \geq t) \leq \exp\left(-\frac{2t^2}{\sum_{i=1}^n c_i}\right).$$

Theorem 12 (Multivariate Lindeberg’s Theorem ([40], Th. 2.27)). *For each n , let $X^{(i,n)}$, $1 \leq i \leq n$, be independent, \mathbb{R}^d -valued random vectors with zero mean and covariance $\Sigma^{(i,n)}$ such that $\sum_{i=1}^n \Sigma^{(i,n)} \rightarrow \Sigma$ (for the Frobenius norm), and Lindeberg’s condition is satisfied:*

$$\forall \varepsilon > 0, \sum_{i=1}^n \mathbb{E} \left[\left\| X^{(i,n)} \right\|^2 I \left\{ \left\| X^{(i,n)} \right\| > \varepsilon \right\} \right] \rightarrow 0 \text{ when } n \rightarrow \infty. \quad (19)$$

Then $S_n = \sum_{i=1}^n X^{(i,n)}$ converges in law toward a centered Gaussian with covariance Σ .

Lemma 13 (Slutsky’s Lemma ([40], Th. 2.7)). *Let X_n, X, Y_n be random variables. If X_n converges in law to X and Y_n converges in probability to a constant c , then (X_n, Y_n) converges in law to (X, c) .*